ADDIS ABABA UNIVERSITY
COLLEGE OF NATURAL SCIENCES
DEPARTMENT OF CHEMISTRY

Solid-State and Quasi-Solid State Photoelectrochemical Solar Energy Conversion based on Polymer PDTSTTz

By: Dawit Tibebu

Advisor: Prof. Teketel Yohannes

June, 2014

Solid-State and Quasi-Solid State Photoelectrochemical Solar Energy Conversion Based on Polymer PDTSTTz

By Dawit Tibebu

A Thesis Submitted to

The Department of Chemistry

Presented in Partial Fulfillment of the Requirements for the Degree of Master of Science in physical Chemistry

Addis Ababa University

Addis Ababa, Ethiopia

June, 2014

ADDIS ABABA UNIVERSITY

SCHOOL OF GRADUATE STUDIES

This is to certify that the thesis prepared by Dawit Tibebu, entitled: *Solid-State and Quasi Solid-State Photoelectrochemical Solar Energy Conversion Based On Polymer PDTSTTz,* submitted in partial fulfillment of the requirement of the degree of master of science in Physical Chemistry compiles with the regulation of the University and meet the accepted standards with respect to the originality and quality.

Signed by the examining committee:

	Signature	Date
Prof. Teketel Yohannes (Advisor)	_____	_____
Prof. Theodros Solomon (Examiner)	_____	_____
Dr. Mesfin Redi (Examiner and Chairman)	_____	_____

_____

Chair of Department or Graduate Program Coordinator

June, 2014

Abstract

The photoelectrochemical properties of a solid-state and a quasi-solid state photoelectrochemical cell (PEC) based on a polymer PDTSTTz and a blend of PDTSTTz:PCBM with an amorphous polymer electrolyte Poly[oxomethylene-olig(oxyethylene)] and ionic liquid complexed with redox couple iodide/triiodide, and oxidized PEDOT as counter electrode were studied.

PEDOT:PSS were spin coated to the substrate and the photo-response of the fabricated device were studied and the followings results were obtained: open-circuit voltage of 311 mV and a short-circuit current of 45.4 μAcm^{-2} and fill factor (FF) 0.34 for the device PEDOT:PSS/PDTSTTz:PCBM/POMOE:I^-_3/I^- at light intensity of 100 $mWcm^{-2}$.

For all devices the photocurrent action spectra of the front and back side were studied and compared. During illumination, a cathodic photocurrent was observed, indicating that the neutral polymer PDTSTTz behaves as a p-type semiconductor. IPCE% ranges from 0.019% to 0.6% from the front side illumination (ITO/PEDOT) were obtained from the different types of device, in addition the Uv-vis absorption spectra of the PDTSTTz film was compared with the photoresponse of the different device and the results were consistent.

Keywords: Photoelectrochemical cell, Conjugated polymer, PDTSTTz, PCBM, PEDOT:PSS

Acknowledgements

I offer my deepest gratitude and special affection to my advisor Prof. Teketel Yohannes for his generous advise, devoted assistance, encouragement in all stages of the work, constant guidance and constructive criticism which were necessary for the progress of the research.

I am very grateful to Ph.D candidates Endale Tsegaye, Bedasa Abdisa and Fedlu Kedir for their excellent sharing of expert knowledge and experiences. Especially Endale Tsegaye provided me with valuable helps in every stage of thesis preparation. I would like to express my sincere thanks to my friends Hagos Tukue and Girma Erjabo who gave me fruitful suggestion during the whole work.

I would like to thank Kotebe University College for sponsoring me to join the school of graduate studies and to all Chemistry Department staffs, for their continuous support during my study.

I greatly appreciate the Addis Ababa University Department of Chemistry, especially Dr. Ahmed Mustafa and staff members for their sincere cooperation during my study.

Finally, I would like to express my sincere gratitude to my beloved family for the support and encouragement I got.

Table of Contents

List of Figures

List of Tables

List of Abbreviations

BMIm	1-butyl-3-methyl immidazolium ion
BP	1-butyl pyridinium ion
CB	Conduction Band
CP	Conjugated Polymer
EDOT	3,4-ethylenedioxythiophene
Eg	Bandgap
EMIm	1-ethyl-3-methyl immidazolium ion
eV	Electron Volt
FF	Fill Factor
HOMO	Highest Occupied Molecular Orbital
IL	Ionic Liquid
IPCE	Incident Photon-to-Current Conversion Efficiency
I_{sc}	Short circuit current
ITO	Indium Doped Tin Oxide
LUMO	Lowest Unoccupied Molecular Orbital
P3HT	Poly-3-hexylthiophene
PCBM	[6,6]-phenyl-C_{61}-butyric acid methyl ester
PDTSTTz	poly[2,6-(4,4‘-bis(2-ethylhexyl)dithieno [3,2-b:2‘,3‘-d]silole)-alt-5,5‘-(3,6-bis[4-(2-ethylhexyl)thienyl-2-yl]-s-tetrazine)]
PECs	Photoelectrochemical cells

PEDOT:PSS	Poly(3,4-ethylenedioxythiophene):poly(styrenesulfonate)
PEO	Polyethylene oxide
POMOE	Poly[oxomethylene-olig(oxyethylene)]
PVP	Polyvinylpyrrolidone
VB	Valence Band
V_{oc}	Open circuit voltage

1. Introduction

Sustainable energy is one of the most pressing issues facing today's society. Access to plentiful, inexpensive, and environmentally benign energy sources would free nations to pursue their greatest human and economic potential. In contrast, continuation along the present energy-consumption path, in which above 80% of our energy is derived from fossil fuels [1], and more than 5% is from nuclear power [2] is not beyond question. In addition, the excessive consumption of fossil fuels during the last few decades have lead to serious environmental problems, primarily due to the emission of green house gases together with many other pollutants, while nuclear power is faced with safety issues and problems associated with radioactive waste disposal. The uneven distribution of fossil fuels in the world is also becoming the cause for conflict among countries [3].

On the other hand, the worldwide power consumption is expected to double in the next three decades because of the increase in world population and the rising demand of energy in the developing countries. As a consequence of dwindling resources, a huge power supply gap of fourteen terawatts is expected to open up by year 2050 equaling today's entire consumption, thus threatening to create a planetary emergency of gigantic dimensions [4].

The increasing public awareness concerning carbon dioxide emissions and the enhanced depletion of fossil fuel reserves motivated the development of environmentally friendly and sustainable energy technologies. Energy is the engine for economic development and that is why sustainable energy sources are the current hot topics in international economics and politics. For sustained economic development we should have sustainable and environmentally friendly energy sources.

Solar energy is one of the promising renewable sources of energy when the supply of the conventional energy sources, such as coal, petroleum, natural gas and nuclear power, gets depleted. The sun provides about 120,000 terawatts to the earth's surface, which amounts to 6000 times the present rate of the world's energy consumption. Energy from the sun is not only available in plentiful supply, but also introduces no direct contamination of the

environment. However, capturing solar energy and converting it to electricity or chemical fuels at low cost and using abundantly available raw materials remains a huge challenge [5, 6].

Ever since the French scientist Edmond Becquerel discovered the photoelectric effect, researchers and engineers have been infatuated with the idea of converting light into electric power. Their common dream is to capture the energy that is freely available from sunlight and turn it into the valuable and strategically important asset that is electric power [7]. Solar cell is a device that converts light energy directly into electrical energy by photovoltaic effect.

The first inorganic solar cell was developed at Bell Laboratories in 1954. It was based on Si and had an efficiency of 6% [4]. Over the years the efficiency has reached greater than 27% for crystalline Si solar cells [9]. In the past twenty years, the demand for solar energy has grown consistently with growth rates of 20–25% per year. However, semiconductor photovoltaics (PVs) still account for less than 0.1% of the total world energy production. The high price of inorganic solar cells limited its use and distribution. The large production cost of silicon for silicon based solar cells lead to long payback times [4]. Therefore, it is wise to search for alternative cheap materials which can be used for fabrication of solar cells.

Owing to their attractive conductivity, inherently conducting polymers have become leading contenders for the development of organic-based solar cells. They provide the possibility of fabricating lightweight, easily prepared, low cost, and flexible solar cells [8]. Photoelectrochemical cell (PEC) is a kind of solar cell that convert light energy directly into electrical energy. In PEC conducting polymer is used as photoactive material.

The photoactive layer of PEC is commonly composed of a blend of a conjugated polymer donor and a fullerene derivative acceptor such as [6,6]-phenyl-C_{60}-butyric acid methyl ester (PC $_{60}$BM) or [6,6]-phenyl-C_{70}-butyric acid methyl ester ($PC_{70}BM$). Regioregular poly(3-hexylthiophene) (P3HT) and $PC_{60}BM$ are the most representative donor and acceptor materials. Nevertheless, the room-temperature mobility for holes (3×10^{-4}

$cm^2V^{-1}s^{-1}$) [10] and higher-lying HOMO energy level (−4.76 eV) of P3HT [11] significantly limits the J_{sc} and V_{oc} values of PECs based on P3HT:PCBM. In a conventional PEC, a liquid electrolyte is used for reduction and oxidation reaction to take place for the mechanism of electron exchange. However, the liquid electrolyte has limitations such as leakage and instability.

In order to improve the visible absorption and decrease the HOMO energy level of conjugated polymers, the use of PDTSTTz as photoactive material in PEC is one possibility. PDTSTTz have a relatively higher-lying HOMO energy level of -5.06 eV and a high hole mobility of 3.56×10^{-3} cm^2 $V^{-1}s^{-1}$ [12]. The results indicate that PDTSTTz is a promising candidate photoactive material for improving the performance of PECs.

The aim of this work is thus, to fabricate and characterize solid state and quasi-solid state PECs consisting of conjugated semiconducting polymer, PDTSTTz, a blends of conjugated semiconducting polymer:PCBM and a blends of conjugated semiconducting polymer:PCBM in the presence of Poly(3,4-ethylenedioxythiophene):poly (styrenesulfonate), PEDOT:PSS film as photoactive electrode, with ion conducting solid polymer electrolyte and ionic liquid complexed with a redox couple. Then, the study helps to examine the effect of fullerene derivative, as an accepter, and PEDOT:PSS, as a hole transporting layer, on the performance of the PECs.

2. Literature Review

2.1 Electronically Conducting Polymers

Until about four decades ago all carbon based polymers were, in general, regarded as electrically non-conducting. They were being extensively used as packaging and insulating materials. However, spectacular developments in the science and technology of synthetic polymers over the past few decades paved the way for the emergence of electrical conductivity as a valued property in polymers [13]. Electrically conducting polymers are those in which their electrical conductivity arises mainly from the existence of sequences of conjugated C=C bonds. Organic conjugated polymers possess interesting electronic and optical properties due to their unique delocalized π-electron systems. The attractions of polymers to the electrical/electronic industries include the ease and low cost of their preparation and fabrication as compared to inorganic semiconductors and metals, especially in films and fibers, and their mechanical properties, particularly flexibility and impact resistance [14].

Although the first inorganic polymer, polythiazyl $(SN)_x$, was discovered in 1975, which possesses metallic conductivity and becomes superconductor at 0.29 K, the idea of using polymers for their electrical conducting properties actually emerged in 1977 with the findings of Shirakawa et. al. [15]. The importance and the potential use of electrically conducting polymer is recognized by the world scientific community when Shirakawa, Heeger and MacDiarmid were laureated in 2000 with the Nobel Prize in Chemistry [16].

Polyacetylene (PA) is a unique material since it is the first polymer which showed electrical conductivity after a process called doping. Intrinsically insulating organic conjugated polymer exhibits increase in electrical conductivity on treatment with oxidizing agent (electron acceptor) or reducing agent (electron donating) agents. When the free-standing films of polyacetylene is exposed to vapors of oxidizing agent (chlorine, bromine, iodine, arsenic pentafluoride) or reducing agent (sodium, potassium, lithium) there will be an increase of twelve orders of magnitude in the conductivity [17].

Based on the experimental finding of polyacetylene, scientists and researchers are motivated and developed other polymers having conjugated π-electron structure

(conjugated polymers), such as polyaniline, (PAni), polypyrrole (PPy), polythiophene (PT), polyfuran (PFu), poly(paraphenylene), polycarbazole and others have been synthesized for exploring them in devices for their possible applications. Figure 1 represents the structures of the repeating units of some conjugated polymers including their common abbreviation.

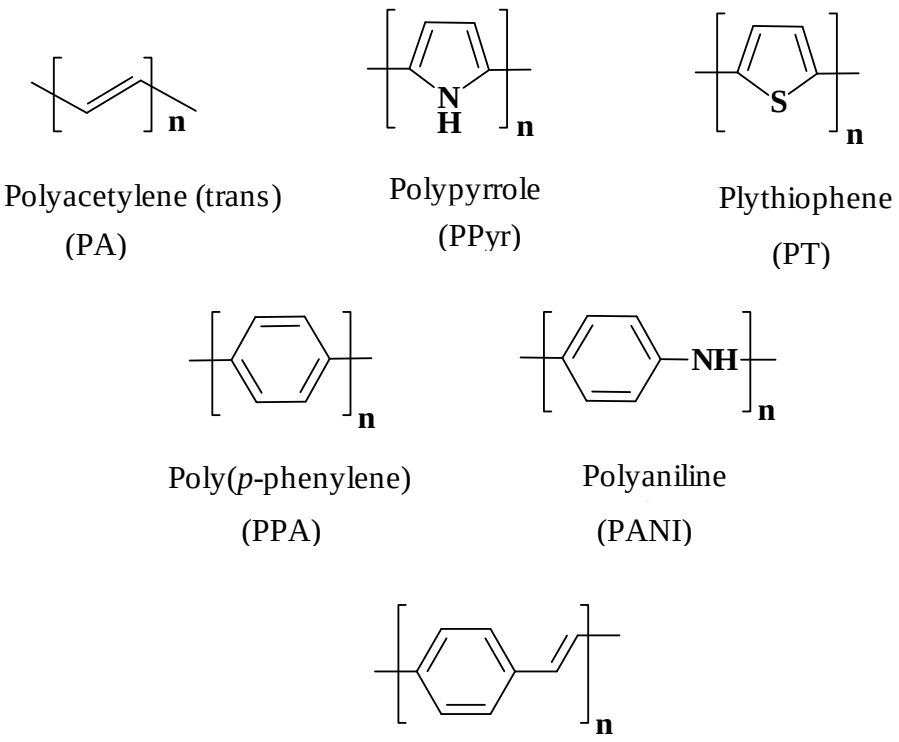

Polyacetylene (trans) (PA)

Polypyrrole (PPyr)

Plythiophene (PT)

Poly(*p*-phenylene) (PPA)

Polyaniline (PANI)

Poly(*p*-phenylene vinylene) (PPV)

Figure 1: Chemical structures of some conjugated polymers.

Conducting polymers are frequently called “synthetic metals” because they present electric, electronic, magnetic and optical properties inherent to metals or semiconductors, while retaining the mechanical properties of conventional polymers. These polymers are being explored for practical applications in electronic and optoelectronic devices such as solar cells, rechargeable battery, electrochromic displays, electromagnetic shielding, sensor technology, and as coatings for corrosion protection, electroluminescent display devices, information storage systems and in communication technology [18, 19].

2.1.1. Doping of Organic Conjugated Polymers

In neutral form conjugated polymers have very low electrical conductivity. Therefore, it is necessary to subject conjugated polymers to a transformation process called "doping" to bring them to conductive state. By doping the conductivity of conjugated polymers increase by up to twelve orders of magnitude. The doping reactions are characterized by charge transfer from the dopant to the polymer or *vice versa*. Depending on the nature of dopant there are two type of doping: p- and n-type. In case of p-type doping the polymer get oxidized whereas in case of n-type doping the polymer get reduced.

$$\text{Polymer} + X \rightleftharpoons (\text{Polymer})^{n+} + X^{n-} \qquad \text{p-type doping}$$

X (electron acceptors/oxidizing agent) = I_2, Br_2, AsF_5

$$\text{Polymer} + M \rightleftharpoons (\text{Polymer})^{n-} + M^{n+} \qquad \text{n-type doping}$$

M (electron donors/reducing agent) = Na, Li, K

The charge on the polymer delocalized along the backbone is formed with a counter ion derived from the dopant. Either p- or n-type doing of polymers are carried out by chemical or electrochemical process during which the number of electrons associated with the polymer backbone change. Therefore, doping agents or dopant are either strong oxidizing or strong reducing agents. The electrical conductivity of the doped material is varied and controlled by the amount of the dopant used.

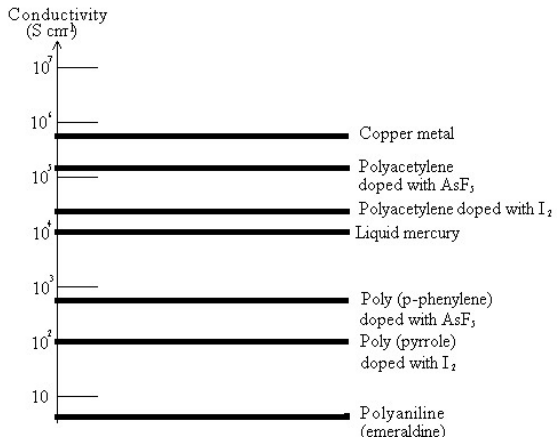

Figure 2: Conductivity ladder of some of the polymers comparing with that of copper [20].

Both n-type which is called reduction (electron accepting-e.g., I_2, PF_6, BF_6, Cl_2, AsF_6) and p-type oxidation or (electron donating-e.g., Na, K, Li, Ca,) dopants have been utilized to induce an insulator-to-conductor transition in electronic polymers. The doping procedures differ from conventional ion implantation used for three-dimensional semiconductors, typically being carried out by exposing the polymer films or powders to vapors or solutions of the dopant, or by electrochemical means.

Polymers such as polyacetylene, polyphenylene, polyphenylenesulfide, polypyrrole, polythiophene and polyaniline can be doped either by chemical or electrochemical methods to achieve conductivity in the range of 1 to 2000 S cm^{-1} [21 - 24].

Besides doping, conductivity highly depends on the temperature, one very important consequence of activated charge transport is that the charge carrier mobility in such a system increases with increasing temperature [25] whereas for metals conductivity increases with decreasing temperature. This is because of the fact that lattice vibrations freeze out as the temperature decreases to absolute zero [26].

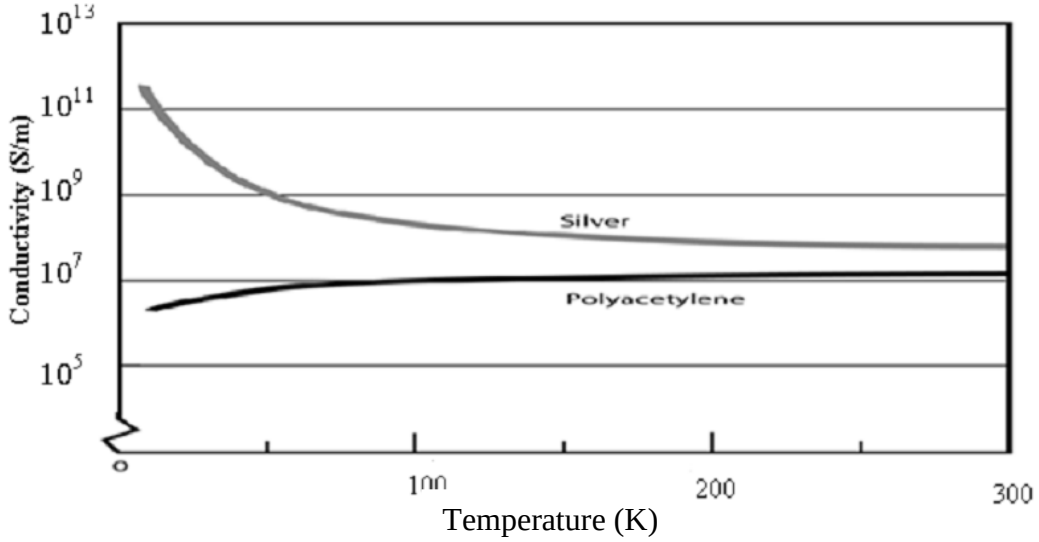

Figure 3: The temperature dependence of polyacetylene and silver conductivity [15].

2.1.2 Charge Carriers

When a large number of atoms, as in the case of metals or semiconductors, are brought together in the crystalline state, the electronic energy levels mix so as to form bands, each band consisting of electronic states with continuous energy levels. Similarly in the case of a polymer when 'n' number of molecules are allowed to interact, 'n' electronic states from each of the π and π* orbitals are formed. If the value of 'n' is very large, as shown in Figure 4, the energy states will be close enough to form a continuous band.

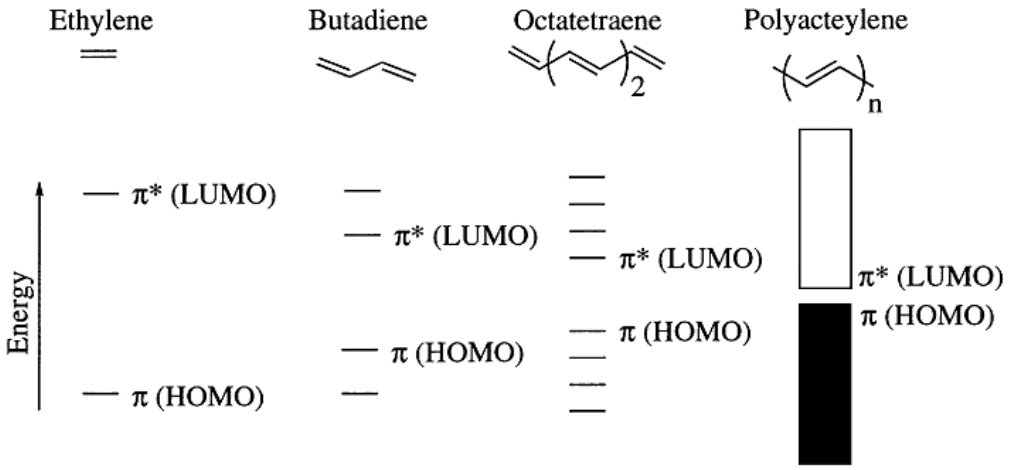

Figure 4: Molecular orbital diagram [14].

The band formed from the HOMO will be entirely full, whereas the band formed from the LUMO will be entirely empty. The highest occupied electronic levels constitute the valence band (VB) and the lowest unoccupied levels, the conduction band (CB). The width of the forbidden band, or band gap between the VB and CB determines the intrinsic electrical properties of the material. In metals there is no range of energies which is deemed unavailable to electrons, which simply means that forbidden gap or band gap in metals is E_g = 0 eV. Consequently metals always have a partially filled free-electron band, because the conduction and valence bands overlap. Hence the electron can readily occupy the conduction band. Insulators have a band gap which is larger than 3 eV

[26]. The electronic properties of metals, semiconductors, and insulators can be differentiated with reference to the energy band gap as shown in Figure 5 below.

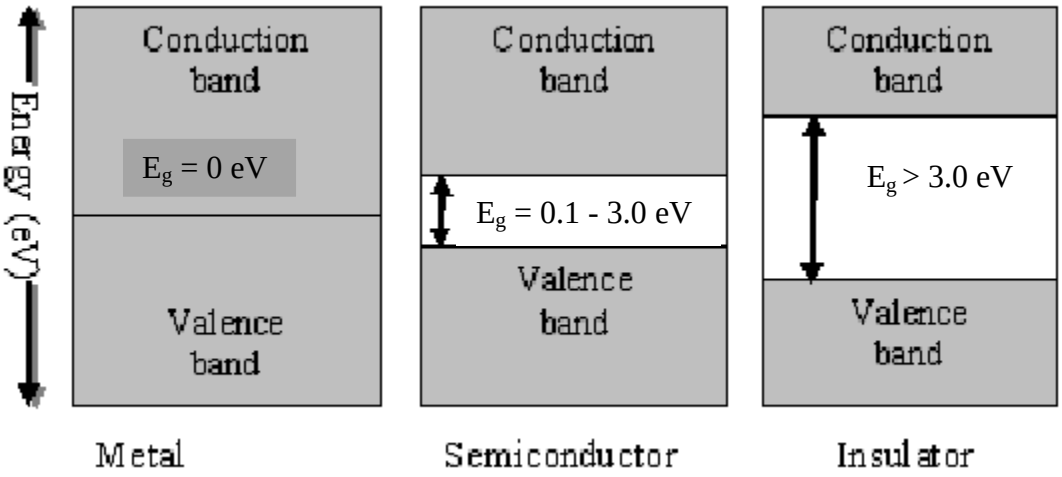

Figure 5 :Energy band diagram demonstrating band gaps [27].

The doping process causes the formation of energy states between the top of the valence band and bottom of the conduction band into the energy gap. The electronic excitation in polymeric materials is accompanied by a distortion or relaxation of the lattice around the excitation, which minimizes the local lattice strain energy. The combined structural and electronic excitation will now look like a defect on the chain. From a chemical point of view, this defect is interpreted as a radical cation or radical anion, whereas, physicists refer to it as a polaron which carries both spin and charge. Removal or addition of a second electron from or to a polaron results in the formation of a bipolaron. The formation of polaron, bipolaron and soliton, in the case of a trans-polyacetylene can be represented as shown in Figure 6. A bipolaron is thus identified as a di-cation or di-anion associated with a strong local lattice distortion. In the case of polymers with degenerate ground state as in the case of polyacetylene, the charges can migrate apart to form solitons. This separation of the charges is possible because a polyene segment of equivalent energy is formed between the charges as they separate [23, 28, 29].

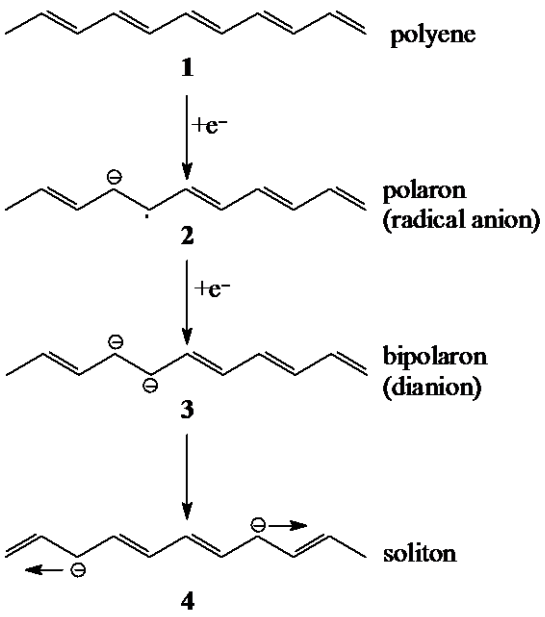

Figure 6: The reduction of trans-polyacetylene to form polaron, bipolaron and soliton.

2.1.3 Charge Transport in Conjugated Polymers

The common electronic feature of many organic polymer is the π-conjugated system, which is formed by the overlap of carbon p_z orbital. Due to the orbital overlap, the π-electrons are delocalized within a molecule and the energy gap between the HOMO and the LUMO is relatively small, i.e. with transition frequencies within the visible range. The low coupling between the molecules in the solid state ensures that the carriers in these materials are strongly localized on a molecule. As shown in Figure 7, transport occurs *via* a sequence of charge transfer steps from one molecule to another, similar to the hopping between defect states in inorganic semiconductors [30].

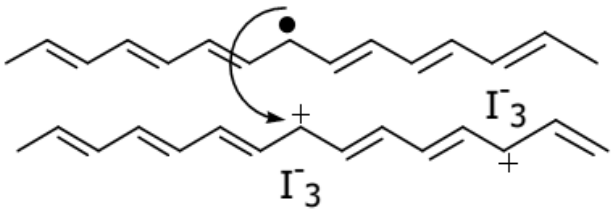

Figure 7: Intersoliton hopping in trans-polyacetylene.

On the basis of both theoretical and experimental studies suggested the low-energy charge-excitations introduced into polyacetylene by light doping are charged solitons. However, these solitons are normally bound to oppositely charged impurities so that soliton conduction is inefficient at room temperature and below. In the presence of both charged and neutral solitons an alternative conduction mechanism is possible: phonon-assisted hopping between the localized electronic mid-gap states associated with the soliton. This is a novel process as it involves hopping between dynamical defects [31].

2.2 Polymers Electrolyte

2.2.1 Solid-State Polymer Electrolyte

Polymer electrolytes are ionically conducting solid phases formed by the dissolution of salts by ion-coordinating macro- molecules, and which in strict terms, are free from low- molecular-weight additives or contaminants. This class of material was first studied by Wright and co-workers' [32] while recognition of the potential of such systems as practical materials for applied electrochemistry, and much of the early development was due to Armand et al. [33].

Polymer electrolytes are complexes of metal salts with high molecular weight polymers containing electron donor atoms or groups of atoms that co-ordinate with the metal ion in the salt. To be successful as a host, a polymer should posses (a) electron donor atoms or groups of atoms (such as -O- ether, -S- sulphide, -N- amine, -P- phosphine, C=O carbonyl, and C≡N cyano) that form co-ordinate bonds with the cations, (b) low barriers to bond rotation for atoms in the main chain so that high flexibility and hence the segmental motion of the polymer chain can take place readily, and (c) a suitable distance between coordinating centers which ensures adequate jumping distance for charge carriers [26].

For the last four decade remarkable international research effort has been dedicated to the development of solvent-free solid polymer electrolytes based on poly(ethylene oxide) (PEO) [32]. As far as electrochemical applications using polymer electrolyte is concerned, PEO is straight forward due to its conductive properties and, like the ease of film formation, excellent complexation with ionic salts, and low glass transition

temperature, it is frequently used in lithium batteries, supercapacitors and photoelectrochromic display devices [34].

Poly (ethylene oxide) (PEO) has been known to exhibit the property to solvate high concentration of ionic salts to give ionic conductivity.

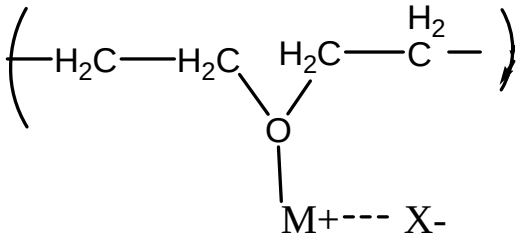

Figure 8: Schematic representation of bond formation of cation and the polymer.

The complexation of ionic salts, which is shown in Figure 8, with PEO has been the subject of active interest in polymer electrolytes, where the weak columbic interaction between the cations and ether oxygen of PEO being the major cause to facilitate ion pair separation. The weak coordination of the polymer PEO with cation served to reduce degree of crystallinity of the polymer PEO (i.e. increase of amorphous region). The increased amorphous region can favor ion transport by the ions to hop from one site to other to improve ionic conductivity [35, 36].

The amorphous structure of the polymer allow easy movement of ions, and must have a flexible chain to assist the ion transport. In PEO the ionic conductivity was found to increase on departing from the stoichiometric ether oxygen to cation ratio (O:M), as the number of vacant sites would increase on increasing the O:M ratio. Figure 9 shows the simplified schematic representation of cation movements in a polymer electrolyte [37].

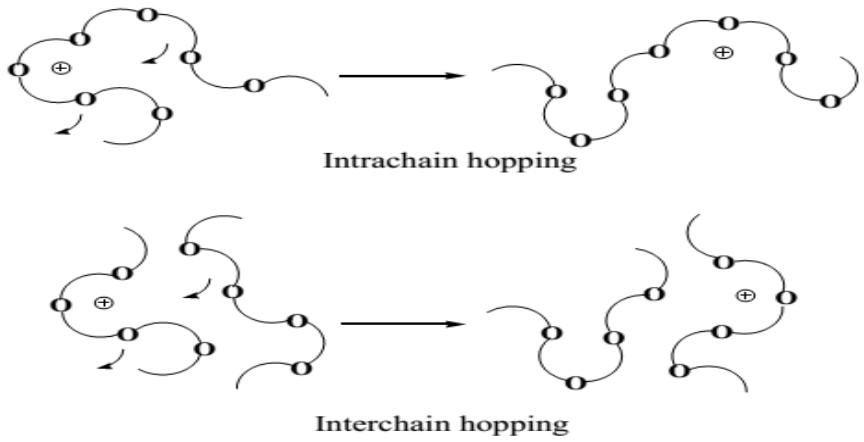

Figure 9: Schematic representation of cation motion in a polymer electrolyte [26].

While polymer electrolytes often exhibit macroscopic mechanical properties which are typical of a solid, a mechanism for short-range ionic motion is provided by local liquid-like relaxation processes at the atomic level. The typical polymer host is poly(ethy1ene oxide), (-CH,CH,O-), known as PEO. This polymer, in its pure form, is chemically and electrochemically stable since it contains only strong unstrained CO, CC and CH bonds. This material, with molecular weight of up to 5 x lo^6, is readily available. A wide variety of salts based on alkali- metal, alkaline-earth-metal, transition-metal and lanthanide ions are soluble in the pure polymer. Polymer electrolytes based on PEO are generally formed by 'solvent casting' method, where solvent is slowly removed from a homogeneous solution of polymer and salt [33]. However a PEO which does suffer from room temperature crystallinity [38]. The polymer chosen for this study is poly[oxymethyleneoligo(oxyethylene)], $CH_2O(CH_2CH_2O)9$, (POMOE), which is effectively a form of PEO. These polymers can be non-crystalline at room temperature, and all have low glass transition temperatures, $T_g = -65^0C$ [39]. The redox couple used to complex with the polymer electrolyte is iodide/triiodide.

2.2.2 Quasi-Solid-State Electrolyte

Potential problems caused by liquid organic electrolytes such as leakage and volatilization of the organic solvent, have had the effect of limiting the long-term performance and practical use of photoelectrochemical solar cell. Solid polymer

electrolytes solved the problems associated with liquid organic electrolyte. However, solid polymer electrolytes such as those based on PEO complexed with suitable ionic salts still have low ionic conductivities and therefore, need to be further optimized in order to obtain electrolytes with reasonably high ionic conductivity to be used in PEC solar cells.

To surmount this problem, solidification and quasi-solidification of the electrolyte have been extensively investigated with various approaches. Among them, ionic liquid electrolytes are prospective substitutes for liquid electrolytes. Since the first report by Walden in 1914 [40], large efforts have been devoted to the investigation of room temperature ionic liquids as green chemistry materials, ILs that consist of organic cations and inorganic anions are attracting wide interest for applications in catalysis, fuel cells, electrochemical capacitors, and batteries due to their non volatility, non flammability, high thermal stability, and high conductivity [3, 41, 42].

In spite of the high viscosity compared to organic solvents, high short-circuit current is revealed in solar cells using ionic liquids due to exchange reaction-based diffusion of an I^-/I_3^- redox couple to the electron transporting processes in various ionic liquids [43]. However, the V_{oc} of the cells with ionic liquids are still lower than those of the cells using organic solvents, which restricts the use of ionic liquids for solar cells. The properties of ionic liquids can be tuned by controlling the structures of the cations and anions. Thus far, most of the studies have been concerned with ionic liquids with iodide anions for the advantage of the high concentration of I^-. However, one disadvantage is their high viscosity resulting in low diffusion coefficients. In Figure 10, some typical cations that are commonly employed in synthesis of ionic liquids are depicts [44].

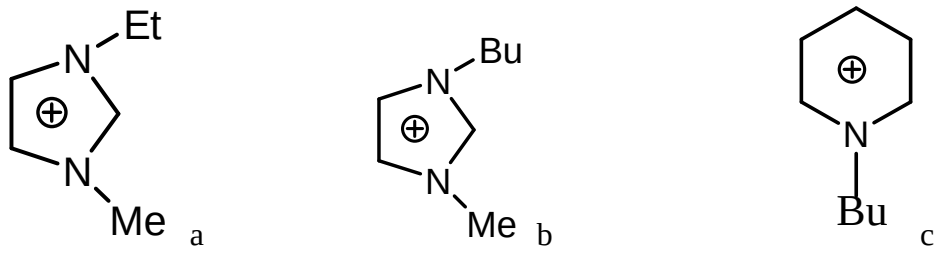

Figure 10: Molecular structure of a) EMIm b) BMIm c) BP.

2.3. Photoelectrochemical Solar Energy Conversion

2.3.1. Introduction

A typical type of the photocurrent - generating device that has a semiconductor in contact with an electrolyte is often referred as photoelectrochemical cells. A photoelectrochemical cell consists of a photoactive semiconductor working electrode (either n- or p -type) and platinum (Pt) coated ITO counter electrode immersed in the electrolyte containing suitable redox couples. If the junction of the semiconductor-electrolyte is illuminated with a light having energy greater than the bandgap of the semiconductor, photogenerated electrons/holes are separated in the space charge region. The photogenerated minority carriers arrive at the interface of the semiconductor-electrolyte. Photogenerated majority carriers accumulate at the backside of the semiconductor. With the help of a connecting wire, photogenerated majority carriers are transported *via* a load to the counter electrode where these carriers electrochemically react with the redox electrolyte [45].

As cited by M. Grätzel [7], Becquerel's pioneering photoelectric experiments in 1839 were done with liquid devices. His research, in which illumination of solutions containing a metal halide salt produced a current between two platinum electrodes immersed in the electrolyte, was motivated by photography [7]. The origin of this photovoltaic phenomenon, called the "Becquerel effect," [46]. It was later found that the photosensitivity can be extended to longer wavelengths by adding a dye to silver halide emulsions. The interest in photoelectrochemistry of semiconductors led to the discovery of wet-type photoelectrochemical solar cells [47].

The PECs that convert light into electricity are termed "electrochemical photovoltaic" or "regenerative cells" and those that generate chemical fuels are "photoelectrosynthetic" or "non-regenerative cells".

Figure 11 shows various types of the photoelectrochemical cells. When shining the light, oxidation reaction will happen on the surface of n-type semiconductors, whilst reduction reaction will happen on the surface of p-type semiconductors. In the electrochemical photovoltaic cell, which is based on a narrow bandgap semiconductor

and a redox couple as shown in Figure 11a, optical energy is converted into electrical energy without change of the free energy of the redox electrolyte (G = 0). The electrochemical reaction occurring at the counter electrode (CE) is opposite to the photo-assisted reaction occurring at the semiconductor working electrode. Thus, they are also called regenerative photoelectrochemical solar cells. If the photogenerated energy is converted to chemical energy, the free energy of the electrolyte will have a change (G ≠ 0). Depending on the relative location of the potentials of the two redox couples (O/R and O'/R' in Figure 11b and c), the photosynthetic cells containing two redox couples, can be further classified as photocatalytic cell (G < 0, Figure 11b) where light merely serves to accelerate the reaction rate and phtoelectrolytic cell (G > 0, Figure 11c) where the cell reaction is driven by light in the contra-thermodynamic direction. Comparing with electrochemical photovoltaic cells, anodic and cathodic compartments need to be separated to prevent the mixing of the two redox couples in these types of cells [48].

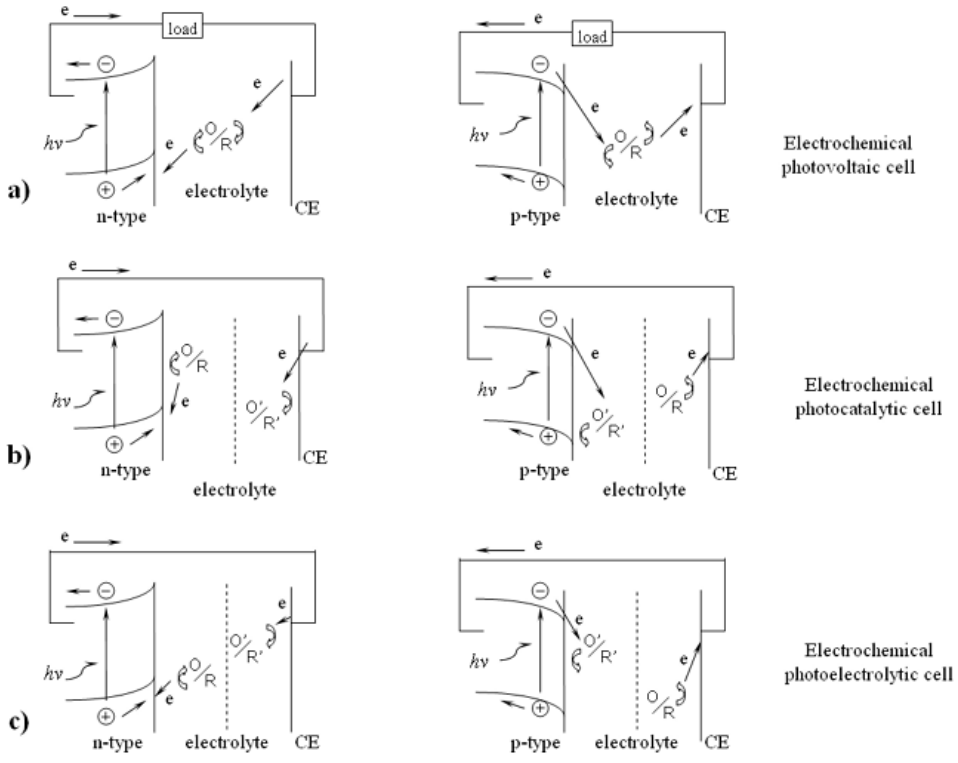

Figure 11: Different types of photoelectrochemical cells with the working electrode (WE) made of semiconductor (n- or p-type) and the counter electrode (CE).

2.3.2. Semiconductor/Electrolyte Interface

All phenomena associated with photoelectrochemical systems are based on the formation of a semiconductor-electrolyte junction when an appropriate semiconductor is immersed in an appropriate electrolyte. The junction is characterized by the presence of a space charge layer in the semiconductor adjacent to the interface with the electrolyte. A space charge layer generally develops in a semiconductor upon contact and equilibration with a second phase whenever the initial chemical potential of electrons is different for the two phases. For semiconductors, the chemical potential of electrons is given by the Fermi level in the semiconductor. For liquid electrolytes, it is determined by the redox potential of the redox couples present in the electrolyte. These redox potentials are also identified with the Fermi level of the electrolyte.

To treat the process occurring in PEC quantitatively, the Fermi level of the semiconductor and that of the electrolyte must be placed on a common energy scale. Using an absolute energy scale, the energy of a redox couple ($E_{f,\ redox}$) is given by Equation 1:

$$E_{f,redox} = E_{ref} - eE_{redox} \qquad (1)$$

In which E_{redox} is the redox potential versus NHE and E_{ref} is the energy of the reference electrode *versus* the vacuum level. The usual value of E_{ref} taken for the NHE is -4.5 eV, although measurements ranges from -4.5 to -4.7 eV. Equation 1 can be rewritten with respect to the vacuum level by Equation 2 [26].

$$E_{f,redox} = -4.5eV - eE_{redox} \qquad (2)$$

If the initial Fermi level in an n-type semiconductor is above the initial Fermi level in the electrolyte (or any second phase), then equilibration of the two Fermi levels (or chemical potentials) occurs by transfer of electrons from the semiconductor to the electrolyte. This produces a positive space charge layer in the semiconductor (also called a depletion layer since the region is depleted of majority charge carriers). As a

result, the conduction and valence band edges are bent such that a potential barrier is established against further electron transfer into the electrolyte as shown in Figure 12.

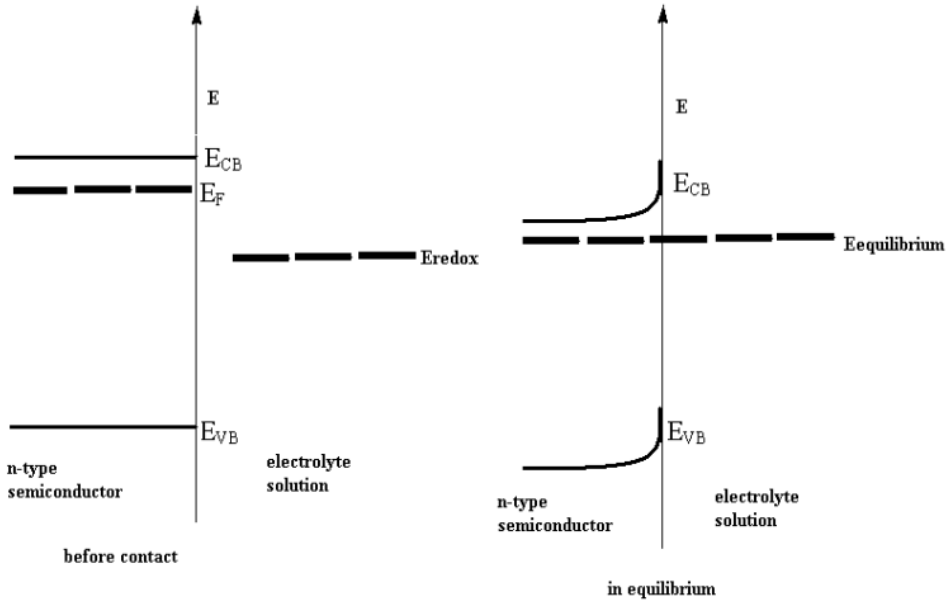

Figure 12: Energetic of an n-type semiconductor-electrolyte solution interface, before contact and at equilibrium.

As shown in Figure 13 the inverse but analogous situation occurs with p-type semiconductors having an initial Fermi level below that of the electrolyte. A negative space charge or depletion layer is formed in the semiconductor, with the valence and conduction bands bending to produce a potential barrier against further positive hole transfer into the electrolyte.

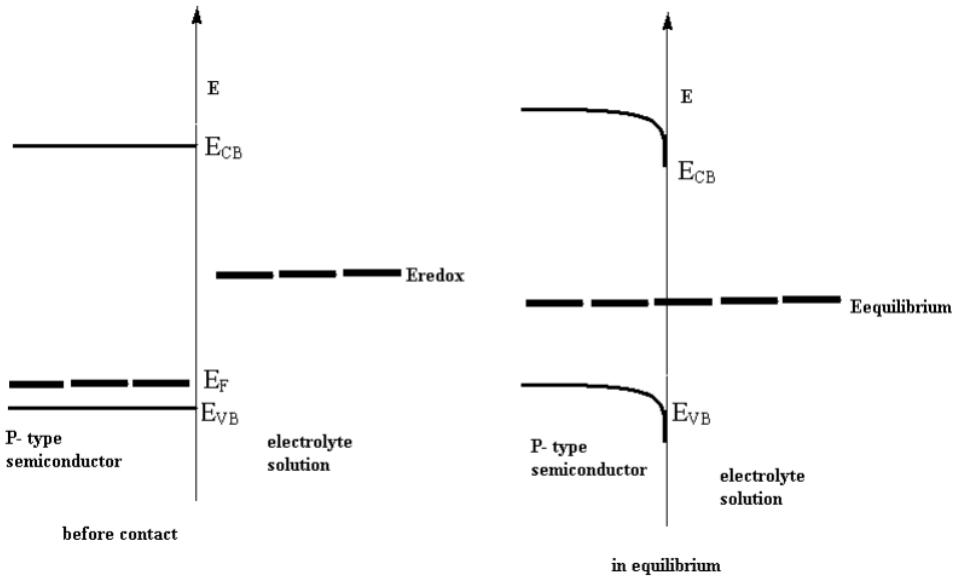

Figure 13: Energetic of a p-type semiconductor-electrolyte solution interface, before contact and at equilibrium.

2.3.3 Conjugated polymers in photoelectrochemical cells

Conjugated polymers are also of interest in the studies of photoelectrochemical cells because of their semiconductor behavior and, as a result, their photoactivity. Besides many other polymers like polyacetylenes, polyaniline (PANI) and polyphenylene-vinylenes (PPV), polythiophenes were of great interest. Even solid electrolytes were applied in photoelectrochemical cells paving a way to all-solid state photoelectrochemical cells [48 - 50]. The working principle of such photoelectrochemical cells is shown in Figure 14. For simplicity the effects occurring at the interfaces described above (bending of conduction and valence band) are neglected in the Figure 14. Due to illumination of the polymer excitons are formed which are electron hole pair bound together. The exiton move to the semiconductor/electrolyte interface and they separate in to a charge carriers. Then the electrons are then transferred to the redox couple, i.e. reducing I_3^- to I^-. When the electrons are transferred further to the back electrode, the former reduced species is oxidized back, leaving no net chemical reaction. The hole left in the valence band is refilled from the front side by transfer of an electron from the ITO electrode to the polymer.

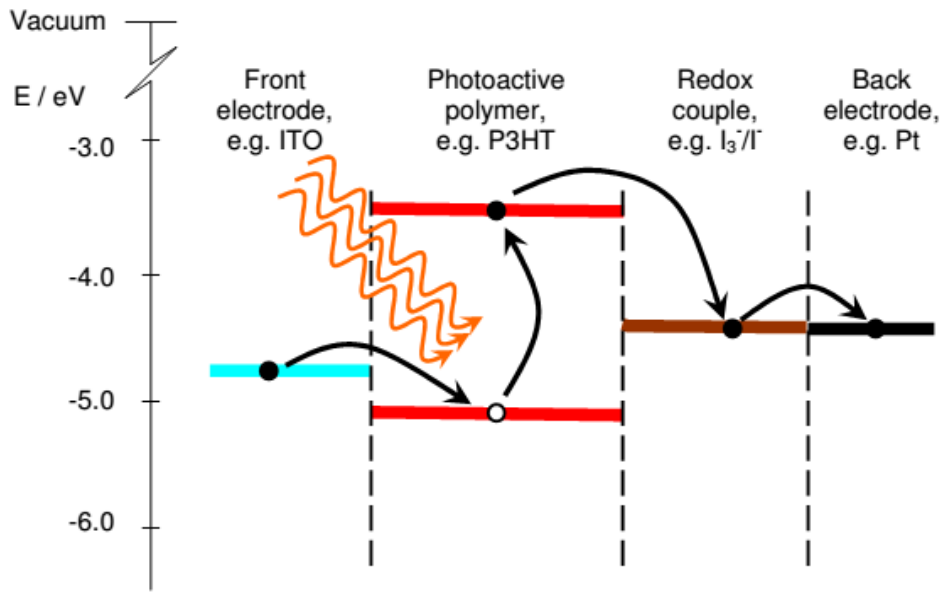

Figure 14: Working principle of a photoelectrochemical cell [37].

2.3.4 Fullerenes in photoelectrochemical cells

The photovoltaic devices based on conjugated polymers have recently been extended by the addition of materials based on photoinduced electron transfer at the contact between two polymers or between a polymer and C_{60} phase. The photoinduced electron transfer at polymer/ C_{60} interfaces has been shown to be extremely fast . Such structures have given much enhanced quantum efficiencies for photon to electron conversion. They rely on the formation of a proper geometry for collection of the photogenerated electron and hole, in two separate phases, to be discharged at electrodes. Such devices give lower open circuit voltages than the metal/polymer contacts in Schottky barrier devices, but more than compensate for this by enhanced photocurrents [51]. From this point of view, conjugated polymers blended with fullerene derivatives which have better light absorption properties could improve the cell' s characteristics.

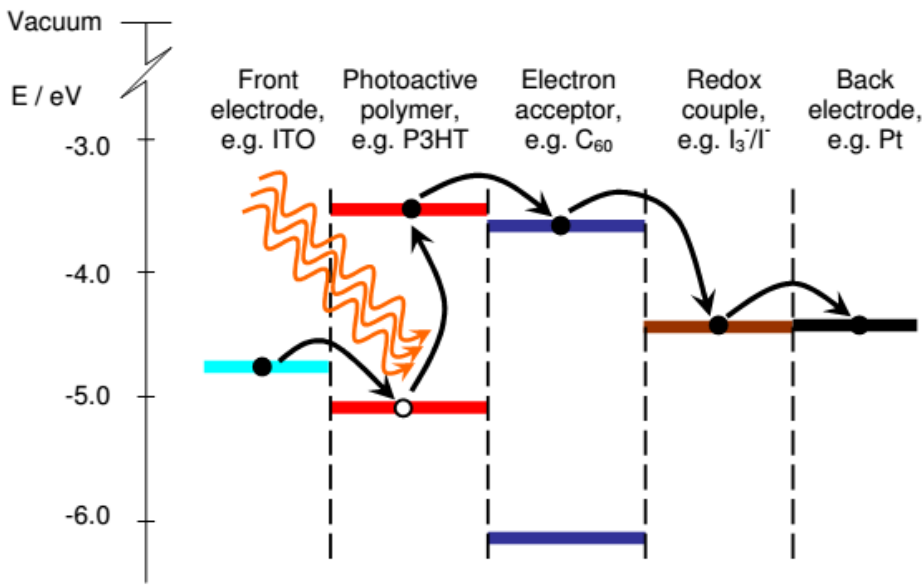

Figure 15: Modification of a photoelectrochemical cell by addition of acceptor materials [37].

Figure 15 shows the working principle of photoelectrochemical cell when acceptor is used. The conduction band of the electron acceptor has to be lower than the photoactive polymer. So the excited electrons can be transferred from the CB of the polymer to the CB of the acceptor and further to the electrolyte. In this study the influence of fullerenes on photoelectrochemical cells based on photoactive polymers is investigated.

2.4. Solar Cell Parameters

The main parameters that are used to characterize the performance of solar cells are the short-circuit current density, J_{sc}, the open-circuit voltage, V_{oc}, the fill factor, FF, and the peak power, P_{max}. To derive the solar cell output parameters that are used for characterization of PEC properties of the device; we shall consider an ideal Schottky diode. Figure 16 shows typical current-voltage characteristics of Schottky diodes in dark and under illumination. When the cell is illuminated, the total current density, J, is equal to the sum of the photocurrent density, J_{ph}, and the dark current density, J_{dark}.

$$J = J_{ph} - J_{dark} \qquad (3)$$

The dark current-voltage characteristics of the solar cell is expressed as

$$J = J_0\left[\exp\left(\frac{qv}{nkT}\right)-1\right] \qquad (4)$$

The I-V characteristics of an illuminated semiconductor is given by

$$J = J_{ph} - J_0\left[\exp\left(\frac{qV}{nkT}\right)-1\right] \qquad (5)$$

Where J is the total current density (dark current density), J_o is the inverse saturation current density which is the current density flowing under sufficiently high reverse bias, q is the charge on an electron, V is the applied voltage, n is the ideality factor of the diode (for an ideal diode n = 1), k is the Boltzmann constant and T is the absolute temperature.

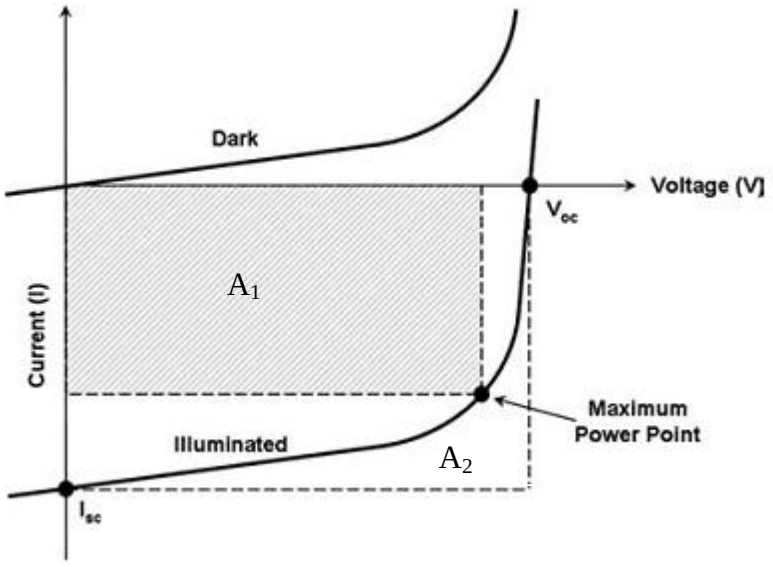

Figure 16: Typical current-voltage characteristics of Schottky diodes in dark and under illumination.

Short-Circuit Current Density

The short-circuit current density, J_{sc}, is the current that flows through the external circuit when the electrodes of the solar cell are short circuited. J_{sc} of a solar cell depends on the

photon flux density incident on the solar cell, that is determined by the spectrum of the incident light. For the standard solar cell measurements, the spectrum is standardized to the AM1.5 spectrum. The maximum current that the solar cell can deliver strongly depends on the optical properties (absorption in the absorber layer and total reflection) of the solar cell. In the ideal case, J_{sc} is equal to the J_{ph} as can be easily derived from Equation 4.

$$J_{sc} = J_{ph} \tag{6}$$

Open-circuit voltage

Open-circuit voltage is the maximum voltage attainable in a solar energy conversion device that can be extracted from an illuminated semiconductor/electrolyte interface. The open-circuit voltage of a solar cell under light is defined as a voltage at which the net current in the cell is equal to zero. This is the condition where voltage is generated but no photocurrent flows. V_{oc} is determined from the current density versus voltage curve as the point at which the curve crosses the voltage axis (J = 0). V_{oc} can be calculated by Equation 7

$$V_{oc} = \left(\frac{nkT}{q} \right) \ln \frac{I_{ph}}{I_0} + 1 \tag{7}$$

Equation 7 shows that V_{oc} depends on the saturation current of the solar cell and the photogenerated current. While J_{ph} typically has a small variation, the key effect is the saturation current, since this may vary by orders of magnitude. The saturation current density, J_o, depends on the recombination in the solar cell.

Fill Factor

Fill Factor (FF) is essentially a measure of quality of the solar cell. It is calculated by comparing the maximum power to the theoretical power (P_T) that would be output at both the open circuit voltage and short circuit current together. In an ideal solar cell all generated charge carriers reach the electrodes and the FF is 1. Due to charge

recombination and resistances within the device not all generated charge carriers reach the electrodes. There are two types of resistance in the solar cell. The serious resistance, R_s, represents the sum of all layer-, contact-, and current-resistances and is the reciprocal slope of the tangent to the I–V curve under open-circuit conditions (Equation 8):

$$R_s = \left(\frac{dV}{dI} \right)_{I=0} \tag{8}$$

The shunt (parallel) resistance, R_{SH}, represents the surface recombination losses, which occur at the different interfaces and leakage currents. R_{SH} is the reciprocal slope of the tangent to the I–V curve under short-circuit conditions (Equation 9):

$$R_{SH} = \left(\frac{dV}{dI} \right)_{V=0} \tag{9}$$

In an ideal solar cell R_s should be minimized ($R_s \rightarrow 0$) and R_{SH} would be maximized ($R_{SH} \rightarrow \infty$). In this case the current density *versus* voltage curve would be rectangular and go along the largest area which is indicated as A_2 in Figure 16. In a real solar cell losses cannot be avoided and the J–V curve is loose its square nature. The point on the J–V curve where the maximum power of the solar cell can be produced is called maximum power point (mp-point). The maximum power point is located on the J–V curve exactly where the product of J and V reaches its maximal value. The area A_1 in Figure 16 indicates this maximal power value. The FF is the relation between those two areas (Equation 10).

$$FF = \frac{A_1}{A_2} \tag{10}$$

The voltage at the maximum power point is V_{mp} and the current density J_{mp}. The FF can be calculated using these values according to Equation 11.

$$FF = \frac{V_{mp} J_{mp}}{V_{oc} J_{sc}} = \frac{P_{\max}}{P_T} \qquad (11)$$

Conversion Efficiency

The conversion efficiency is calculated as the ratio between the generated maximum power and the incident power. The irradiance value, P_{in}, of 100 mW/cm^2 of AM1.5 spectrum has become a standard for measuring the conversion efficiency of solar cells.

$$\eta = \frac{p_{out}}{I_{in}} = \frac{V_{mp} J_{mp}}{I_{in}} = \frac{V_{oc} J_{sc} FF}{I_{in}} \qquad (12)$$

Incident Photon to Current Conversion Efficiency (IPCE)

The incident photon to current conversion efficiency (IPCE) or external quantum efficiency (EQE) is the ratio of the number of charge carriers collected by the solar cell to the number of photons of a given energy shining on the solar cell from outside (incident photons) at a certain wavelength (Equation 13).

$$IPCE\% = \frac{1240 J_{sc}(\mu A / cm^2)}{\lambda(nm) I_{in}(W / m^2)} \qquad (13)$$

where J_{sc} is the short-circuit current density for monochromatic irradiation, and λ and I_{in} are the wavelength and the intensity, respectively, of the monochromatic light. If IPCE is 100%, every absorbed photon injects an electron into the circuit. IPCE is a measure for the absorption quality of the solar cell at a certain wavelength combined with its charge transport quality. If, e.g., the cell absorbs all incident photons at a certain wavelength but the charges cannot travel to the electrodes due to recombination, the IPCE nevertheless will be zero. Hence, the IPCE correlates often to the absorption spectrum of the active layer but a strong deviation cannot be excluded [37, 52].

3. Objectives

3.1. General Objectives

The general objective of this study is to fabricate and characterize conducting polymer based solid state photoelectrochemical cells, quasi-solid state photoelectrochemical cells solar energy conversion, and the effect in the performance after the introduction of PEDOT:PSS into PDTSTTz/PCBM system as a hole transporting layer.

3.2 Specific Objectives

The specific objectives include:

- To produce all-solid-state photoelectrochemical solar cells using conjugated polymer PDTSTTz as photoactive materials and study the PEC properties of the cell with basic structure: ITO/PDTSTTz / POMOE:I^-_3/I^-/PEDOT/ ITO.
- To produce all-solid-state photoelectrochemical solar cells using conjugated polymer PDTSTTz:PCBM as photoactive materials and study the PEC properties of the cell with basic structure: ITO/PDTSTTz:PCBM / POMOE:I^-_3/I^-/ PEDOT/ ITO.
- To study the effect of introducing PEDOT:PSS in all-solid-state photoelectrochemical solar cells using conjugated polymer PDTSTTz:PCBM as photoactive with basic structure: ITO/PEDOT:PSS/PDTSTTz :PCBM/ POMOE:I^-_3/I^-/ PEDOT/ ITO.
- To produce Quasi-solid state photoelectrochemical solar cells using conjugated polymer PDTSTTz as photoactive materials and study the photovoltaic properties the cell with basic structure: ITO/PDTSTTz /IL:I^-_3/I^-/PEDOT/ITO.
- To produce Quasi-solid state photoelectrochemical solar cells using conjugated polymer PDTSTTz:PCBM as photoactive materials and study the photovoltaic properties the cell with basic structure: ITO/PDTSTTz:PCBM /IL:I^-_3/I^-/PEDOT/ ITO.
- To characterize the solar cells using various standard characterization techniques such as I-V, IPCE, Uv-vis and transient study.

4. Experimental

4.1 Materials, Chemicals and Equipment

The materials that we used for the fabrication of the PECs are PDTSTTz and PCBM (from SOLENE) as photoactive materials, PEDOT:PSS (Bayerton PH) as hole conducting layer, and amorphous poly(ethylene oxide), POMOE with a repeating unit of $CH_2O(CH_2CH_2O)_9$ and a redox couple KI/I_2 as a polymer electrolyte and EMIm-I and PVP(Aldrich), as Quasi-Solid state electrolyte. To produce PEDOT film on ITO by electropolymerization, EDOT solution (Bayer) was used. ITO-glass coated with PEDOT is used as a counter electrode. 1,2-dichlorobenzene (Riedel-de Haen) was used as a solvent for dissolving both the donor polymer and acceptor material. Other solvents and chemicals used were methanol (Fluka), acetonitrile (Aldrich), sodium iodide (BDH), KI (BDH), I_2 (Aldrich), acetone (Aldrich) and isopropyl alcohol (Riedel-de Haen).

All mass measurements were done with a digital balance, Denver instruments (Model XE-50). The J-V measurements was done by an Oriel power supply (Model 66182) with the presence of CHI630 electrochemical analyzer and the white light intensity was calibrated with a Gigahertez-optik optometer with RW-37; single channel radiometric and photometric detector heads (Model X1-1). A grating monochromator (Model 77250) was used for wavelength selection. The spectra were corrected for the spectral response of the lamp and the monochromator by normalization to the response of a calibrated Silicon photodiode (Hamamatsu, model S-1336-8BK). Optical absorption measurements were carried out using Spectroscopic GENSEYS 2PC Uv-vis spectrometer.

The chemical structures of the conjugated polymers, the acceptor molecule, the counter electrode active layer and hole transporter used in this work are depicted in Figure 17.

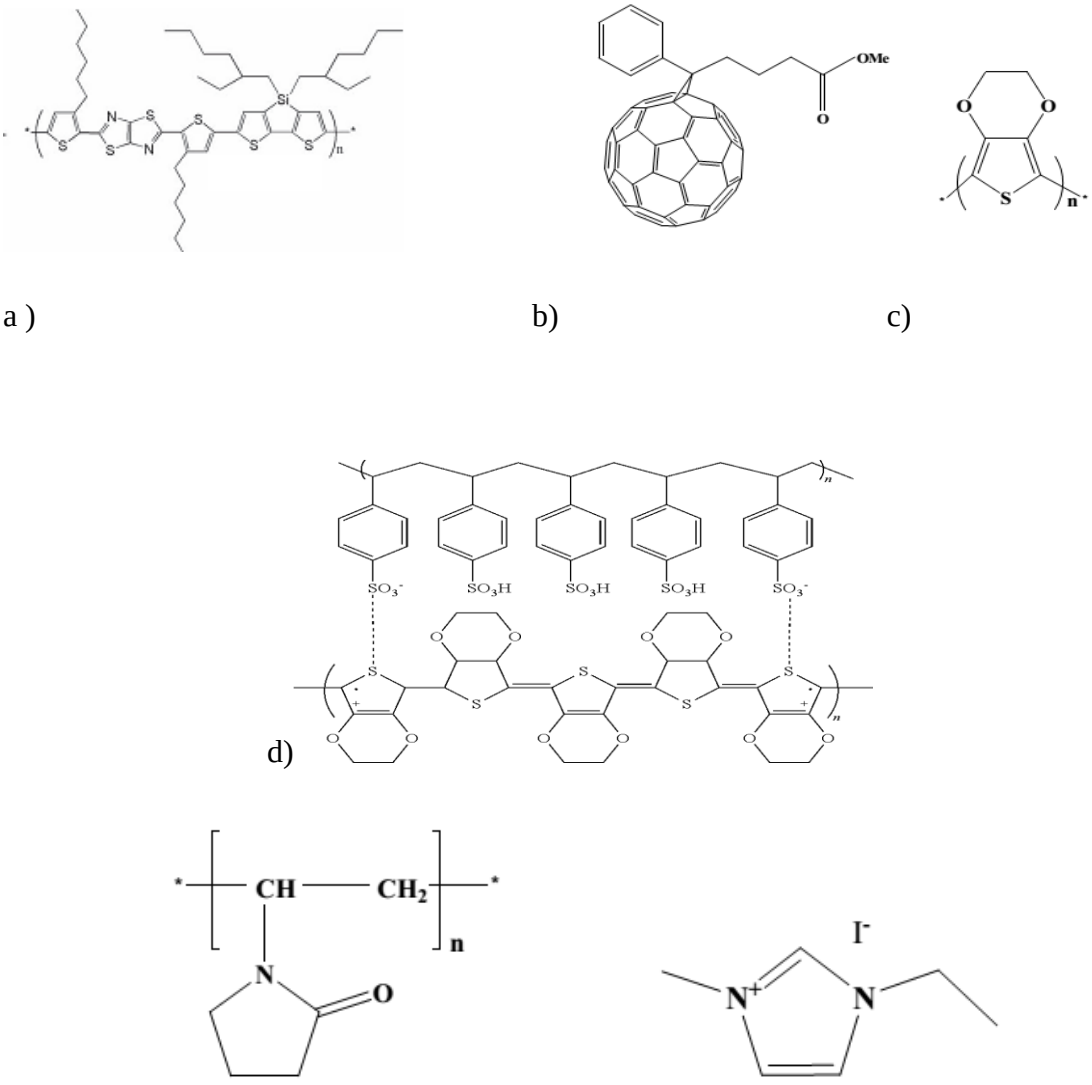

a) b) c)

d)

e) f)

Figure 17: Chemical structure of a) PDTSTTz b) PCBM c)PEDOT d) PEDOT-PSS e) PVP f) $EMImI^-$

4.2 Preparation of Substrate and Solution

4.2.1. Preparation of ITO-Coated Glass

ITO-coated glass having transmittance about 82% - 89% [53] in the visible region of the solar spectrum was employed as a substrate for the photoactive materials and counter

electrodes. It was cleaned successively with detergent, acetone and 2-propanol in Ultrasonic bath, then rinsed with distilled water and dried with an air gun [51].

4.2.2. Preparation of Solution and Photoactive Electrode

A solution of 2.5 mg PDTSTTz in 1 mL of 1,2-dichlorobenzene was prepared for donor only type of photoactive electrode and a mixture of 2.5 mg PDTSTTz and 2.5 mg PCBM in 1 mL of 1,2-dichlorobenzene was prepared for a PEC. The photoactive film was formed by drop casting the prepared solution on a pre-cleaned ITO-coated glass. The third type of photoactive layer was prepared by spin-coating PEDOT:PSS with 4000 rpm on ITO-coated glass and annealed at 140^{o}C on a hotplate for 15 minutes and then drop casting the mixture solution [54].

4.2.3. Preparation of the Counter Electrode

In PEC, since bare ITO is irreversible for iodide/triiodide oxidation/reduction reaction, it is coated with a material capable of catalyzing the redox reaction in the electrolyte. Yohannes et al. [55] has shown that PEDOT improved the charge transfer between ITO and iodide/triiodide redox couple in photoelectrochemical solar cell. In our study PEDOT has been used to improves the charge transfer between ITO and the iodide/triiodide redox couple. It was formed by electrochemical polymerization of EDOT in a three electrode one-compartment electrochemical cell. The electrochemical cell consisted of a pre-cleaned ITO-coated glass working electrode, platinum foil counter electrode, and quasi-Ag/AgCl reference electrode dipped in acetonitrile solution. The solution used for the polymerization contained 0.2 M EDOT and 0.1 M Tetrabutylammonium tetrafluoroborate in acetonitrile. The polymerization was carried out potentiostatically at +1.8 V for 5 s. At this potential, the electrode surface becomes covered with blue-doped PEDOT film. The cell was then rinsed with acetonitrile and dried in air [37].

4.2.4. Preparation of the Electrolyte

4.2.4.1. Preparation of the Solid State Electrolyte

The polymer electrolyte was prepared by dissolving 318.2 mg of POMOE in 25 mL of methanol. The redox couple I_3^-/I^- was prepared by dissolving 49.58 mg KI and 7.58 mg I_2

separately in 25 mL of methanol. Finally, equal volume of each of the above three solutions were mixed to produce the polymer electrolyte complexed with a redox couple. The mole ratio of oxygen to potassium as calculated by taking into account both the oxymethylene and oxyethylene oxygen atoms was 25 and the mole ratio of KI to I_2 was 10, i.e., the concentration of I_2 is one-tenth the concentration of KI. The ionic conductivity of POMOE is known to be high at room temperature when the oxygen to cation (potassium) mole ratio is 25 [51] .

4.2.4.2 Preparation of the Quasi-Solid State Electrolyte

The polymer gel electrolyte was prepared by taking 0.9 M of EMIm-I and add into acetonitrile under stirring to form a homogeneous liquid electrolyte. In order to obtain a better conductivity, 0.5 M of sodium iodide was dissolved in the above homogeneous liquid electrolyte, and then 0.12 M iodine and 35% (w/w) of PVP were added. Then, the resulting mixture was heated at 80^0C under vigorous stirring to dissolve the PVP polymer, followed by cooling down to room temperature to form a gel electrolyte [56].

4.3. PEC Assembly

Finally, both the solid and quasi solid polymer electrolyte complexed with I_3^-/I^- was deposited in the form of thin film by drop casting on top of all types of photoactive electrode coated on ITO glass and allowed to dry in a laboratory atmosphere. The PEC was completed by pressing against PEDOT coated ITO-glass as counter electrode [51].

The devices were then mounted in a sample holder inside a metal box having a 1 cm^2 light entrance window, which determine the illumination area. All experiments were carried out at ambient temperature.

The basic device structure of solid-state PEC used in this study is shown in Figure 18.

Figure 18: The basic structure of the solid-state PEC.

4.4. Experimental Set-Up and Measurement

A schematic of the experimental set-up used to measure the photoelectrochemical properties of the device is shown in Figure 19. A 250 W tungsten-halogen lamp regulated by an Oriel power supply is used to illuminate the PEC. The resulting photoelectrochemical properties were studied using electrochemical Analyzer. The white light intensity was measured in the position of the sample cell with an optometer. A grating monochromator was used to select a wavelength manually between 300 nm and 800 nm at an interval of 10 nm and the photocurrent was measured at each wavelength.

The spectra were corrected for the spectral response of the lamp and the monochromator by normalization to the response of a calibrated Silicon photodiode.

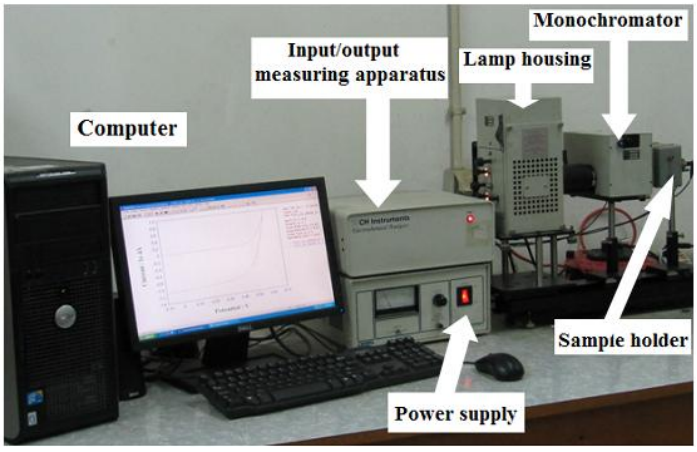

Figure 19: General experimental set-up for the photoelectrochemical measurements.

5. Results and Discussion

5.1. Current-Voltage Characteristics

The current is measured as a function of the applied voltage, both in the dark and under illumination with light intensity of 100 mWcm^{-2}. The measured data allows to determine the J_{sc}, the V_{oc}, and the FF of the device. Figure 20, 21, and 22 shows the current-voltage characteristic of the PECs based on a PDTSTTz, a blend of PDTSTTz:PCBM and a blend of PDTSTTz:PCBM on PEDOT:PSS respectively. All the devices were illuminated from their front sides (ITO|PEDOT).

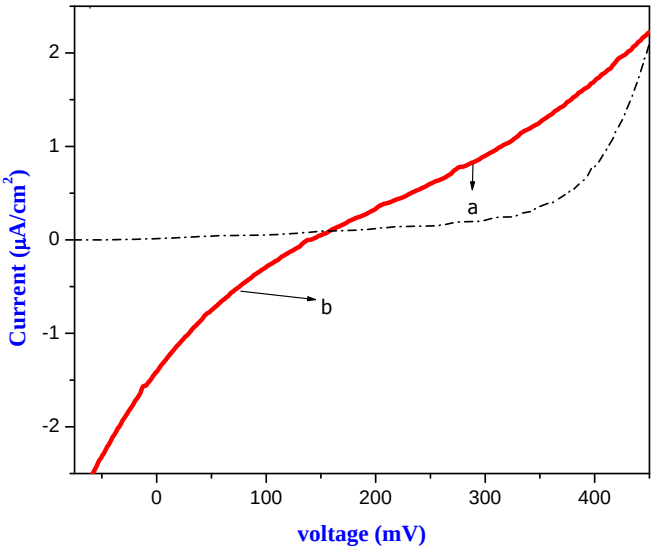

Figure 20: Current density-Voltage characteristics of ITO/PDTSTTz/POMOE:I_3^-/I^-/ PEDOT/ITO a) in the dark b) under illumination of 100mWcm^{-2}.

In the dark, the current was negligible and remained relatively constant in the negative potential range while a larger anodic current was observed in the larger positive potential range. The positive applied potential acts to diminish the effects of the internal barrier field that is set at the polymer/electrolyte junction. As a result, charge carriers acquire enough energy to cross the barrier, resulting with large anodic currents. On the other hand, applying a negative potential enhances the barrier potential and only a small current flows [57], which indicates that the cells have desirable photoelectrochemical.

Under illumination, a cathodic photocurrent was generated, which is characteristic for p-type semiconductors. The incident light produced a short circuit photocurrent and an open circuit phtovoltage which are shown in Table 1.

Illumination of the polymer in the PEC creates excitons, which are electron-hole pairs bound together. The photocurrent results from diffusion of the excitons to the semiconductor polymer electrolyte interface, where they dissociate into free carriers that migrate to opposite electrodes. Electrons move to the front contact and holes to back contact as expected for p-type semiconductors. The electrons generated reduce the tri iodide to iodide and the iodide formed will give its electron to counter electrode and oxidized back to triiodide. The electron will flow through the external circuit and combine with hole. Hence, there is no net chemical reaction taking place and therefore, the PEC converts the optical energy into electrical energy. The dissolved redox couple provides chemical species that can rapidly exchange charge between the anode and the cathode so that current can flow through an external load.

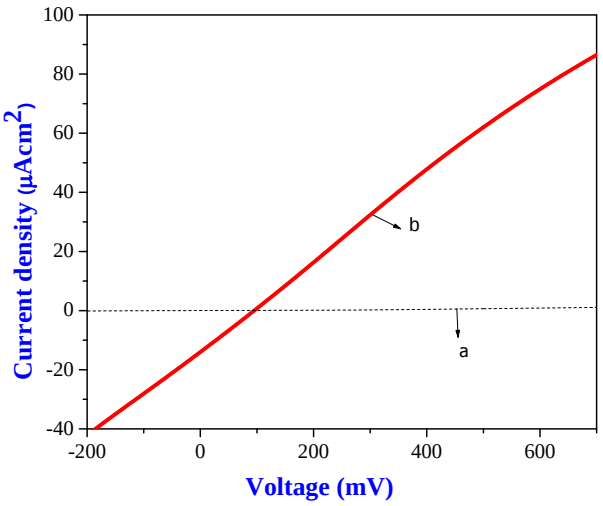

Figure 21: Current density-voltage characteristics of ITO/PDTSTTz:PCBM /POMOE:I_3^- /I^-/ PEDOT/ITO a) in the dark b) under illumination of 100mWcm^{-2}.

Similar actions were observed for PDTSTTz:PCBM based solar cell. The photogenerated electron transfer from p-type conjugated polymer to PCBM, since the LUMO of the

acceptor PCBM is lower than that of the donor PDTSTTz, the photoexcited electrons would relax into the PCBM LUMO and separate from the holes. This electron transfer is known to take place ~1000 times faster than any decay of the photo excitation [58]. Thus, the increase of J_{sc} is related to the better charge transfer in PDTSTTz:PCBM composite electrode. This phenomenon increases the dissociation of the exciton into electron and hole and hence increased the photocurrent of the PEC based on the blend of PDTSTTz and PCBM with a decrease in V_{oc}. One of the reason for the decrease in V_{oc} is that, it depend on the HOMO of the donor and the LUMO of the accepter which is lower in energy than the LUMO of the donor [59]. Hence, the results show that PDTSTTz:PCBM composite photoactive electrode has larger J_{sc} and smaller V_{oc} as compared to the cell composed of pure PDTSTTz.

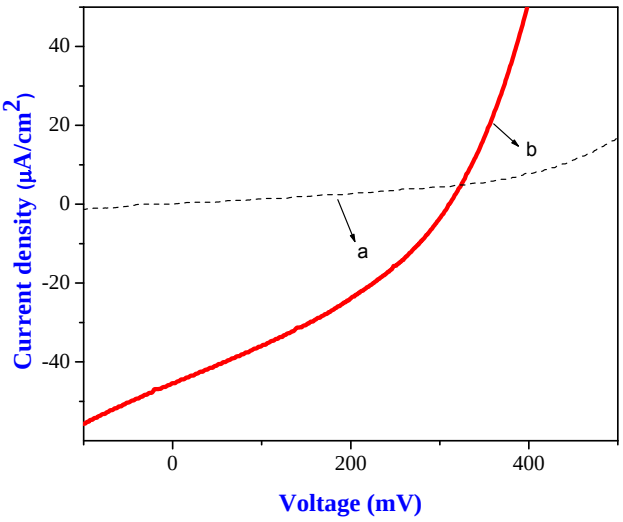

Figure 22: Current-voltage characteristics of ITO/PEDOT:PSS/ PDTSTTz:PCBM /POMOE:I_3^-/I^-/ PEDOT/ITO a) in the dark b) under illumination of 100mWcm^{-2}.

As known from other studies, ITO has variable work function ranging from 4.1 – 5.1 eV. ITO also has a large surface roughness. The spikes on the rough surface of ITO can cause current leakage mechanisms and there by increases recombination of holes and electrons. The increased recombination will decreases open-circuit voltage. Therefore, it is important to smooth the rough surface of ITO. To counter the above issues, intermediate

polymer layers have been considered such as poly(3,4-ethylenedioxythiophene) blended with polystyrenesulfonate PEDOT:PSS [60].

PEDOT:PSS film has high transparency in the visible range, high mechanical flexibility, and excellent thermal stability [61] and is one of the best hole-conducting buffers because its ionization potential is close to the work function of ITO, whereas its electron affinity is sufficiently low to block electrons [62].

As shown in Figure 22 a device with the presence of PEDOT:PSS show best diode behavior with a great enhancement of both in J_{sc} and V_{oc} which is probably the presence of PEDOT:PSS minimizes the roughness of the ITO surface and facilitates the hole conductivity in to ITO layer and again which reduces recombination and resulted in an increase the J_{sc}.

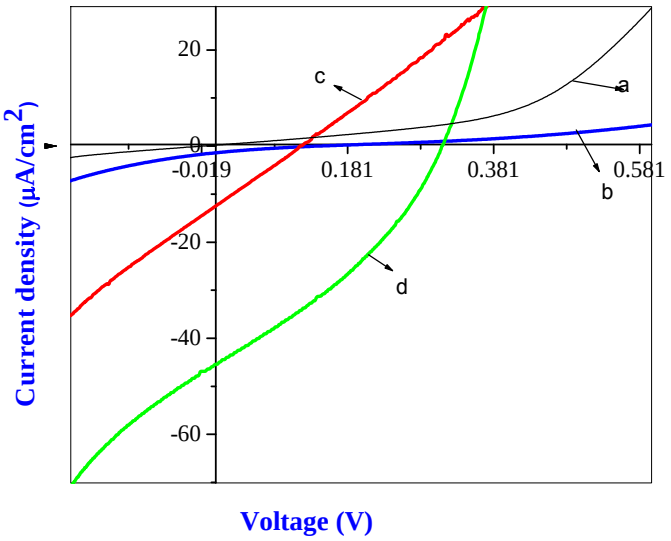

Figure 23: Current density-voltage characteristics of a cell where a) in the dark b)ITO/PDTSTTz/POMOE:I_3^-/I^-/ PEDOT/ITO c) ITO/PDTSTTz:PCBM/POMOE:I_3^-/I^- /PEDOT/ITO d) ITO/PEDOT:PSS/ PDTSTTz:PCBM /POMOE:I_3^-/I^-/PEDOT/ITO under illumination.

On the other hand, minimizing the roughness of the ITO surface reduces the series resistance which is related with contact and, therefore there is an increment in J_{sc} and FF . The results obtained revealed that the multi-layered structure of the device with the PEDOT:PSS can improve PEC performances. Figure 23 shows the comparison of the current-voltage characteristics of the different types of PEC cells based on all solid state polymer electrolyte under illumination with 100 $mWcm^{-2}$. The current density - voltage characteristics of the different devices shown in Figure 23 clearly demonstrates the importance of PEDOT:PSS in improving the performance of PEC.

The summary of the results given in Table 1 shows that for polymer only PEC, J_{sc} = 1.4 μAcm^{-2} and V_{oc}=139 mV were obtained. When polymer:PCBM blend is used the short-circuit current increased and the open-circuit voltage decreased (J_{sc} = 12.5 μAcm^{-2} and V_{oc}=115 mV). Moreover, when ITO with film PEDOT:PSS and polymer:PCBM blend is used both short-circuit current and open-circuit voltage improved (J_{sc} = 45.4 μAcm^{-2} and V_{oc} = 311 mV).

Table 1: Photoelectrochemical properties for the solid state PECs under the same illumination condition.

Photoactive electrode	**V_{oc} (mV)**	**J_{sc} ($\mu A/cm^2$)**	**FF**
PDTSTTZ /POMOE: I^-_3/I^-	139	1.4	0.20
PDTSTTz:PCBM/ POMOE: I^-_3/I^-	115	12.5	0.25
PEDOT:PSS/PDTSTTz:PCBM / POMOE: I^-_3/I^-	311	45.4	0.34

The other type of polymer electrolyte used in this thesis is a quasi-solid polymer electrolyte with redox couple I^-_3/I^-. Figure 24 and 25 shows the current density - voltage characteristic of the PECs based on a PDTSTTz and a blend of PDTSTTz:PCBM with a quasi-solid polymer electrolyte in the dark and under illumination of 100 $mWcm^{-2}$, respectively. The devices were again illuminated from their front sides (ITO|PEDOT).

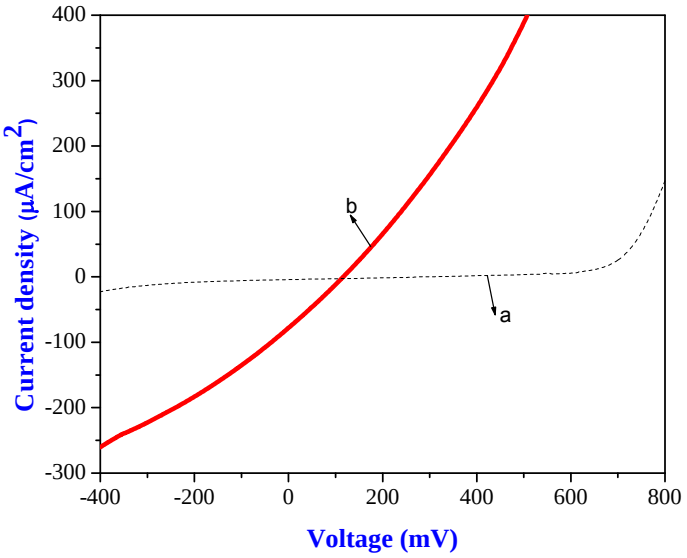

Figure 24: Current density - voltage characteristics of ITO/ PDTSTTz /IL/PEDOT/ITO a) in the dark b) under illumination of 100mWcm^{-2}

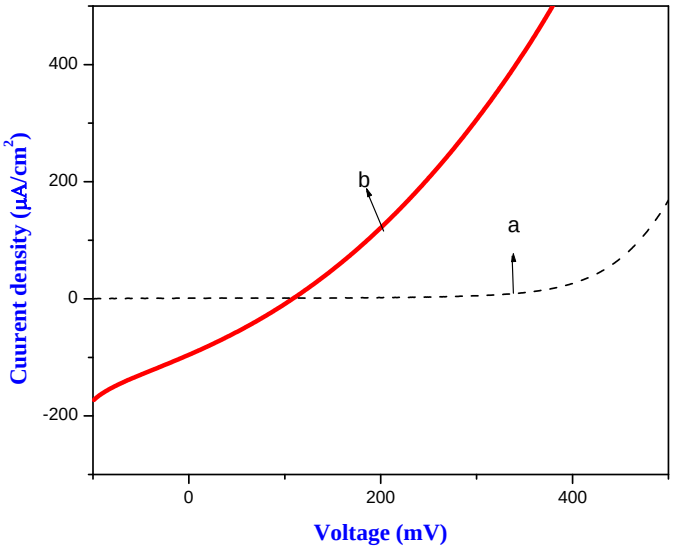

Figure 25: Current density - voltage characteristics of ITO/ PDTSTTz:PCBM /IL/ PEDOT/ITO a) in the dark b) under illumination of 100mWcm^{-2}.

Figure 26 shows the comparison of the current-voltage characteristics of the different types of PECs based on quasi-solid state polymer electrolyte under illumination with 100 $mWcm^{-2}$.

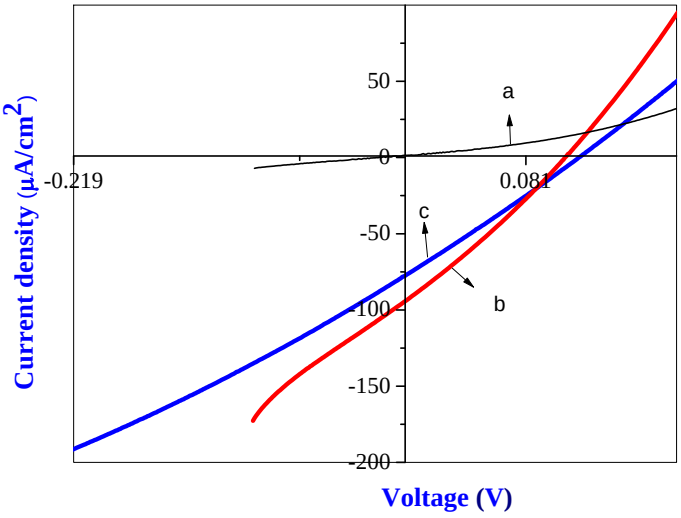

Figure 26: Current density - voltage characteristics of a) in the dark b) under illumination for ITO/ PDTSTTz /IL/ PEDOT │ITO c) under illumination for ITO/ PDTSTTz:PCBM /IL/PEDOT/ITO.

Under illumination, a cathodic photocurrent was generated, which is characteristic for p-type semiconductors. The incident light produced a short circuit photocurrent and an open circuit voltage which are shown in Table 2 including the calculated fill factor.

Table 2: Photoelectrochemical properties for the Quasi -solid state PECs under the same illumination condition.

Photoactive electrode	**V_{oc} (mV)**	**J_{sc} (μA/cm^2)**	**FF**
PDTSTTz /IL	116	78.5	0.26
PDTSTTz:PCBM /IL	107	95.6	0.28

From table 2, high short-circuit current is revealed in PECs using ionic liquids. This is explained by high conductivity of the IL and a fast charge transport based on the exchange diffusion reaction of an I_3^-/I^- redox couple to the electron transporting processes in ionic liquids.

In all measured devices, the shape of the current density - voltage curve and the fill factor reflects the charge transfer resistive character of the electrolyte.

5.2 Photocurrent Action Spectra

The photocurrent action spectrum plotted in terms of IPCE% *versus* wavelength under front- and backside illumination conditions for the different types of PECs are shown in Figure 27.

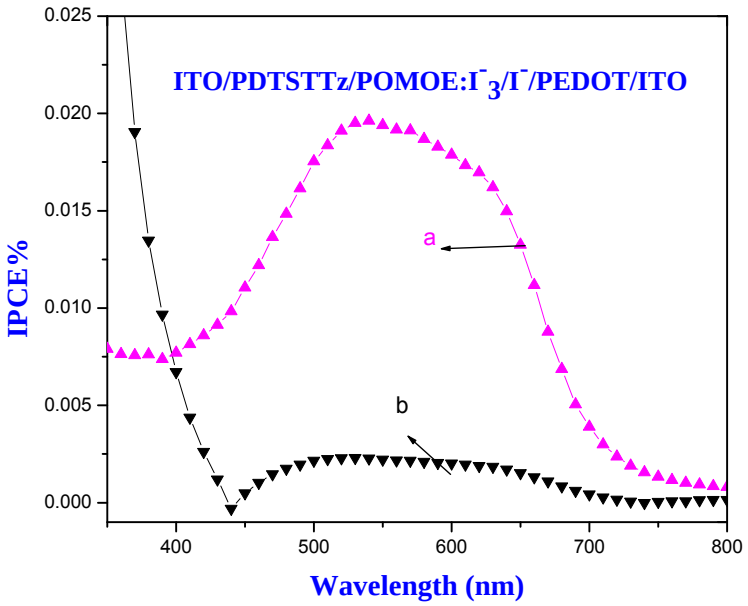

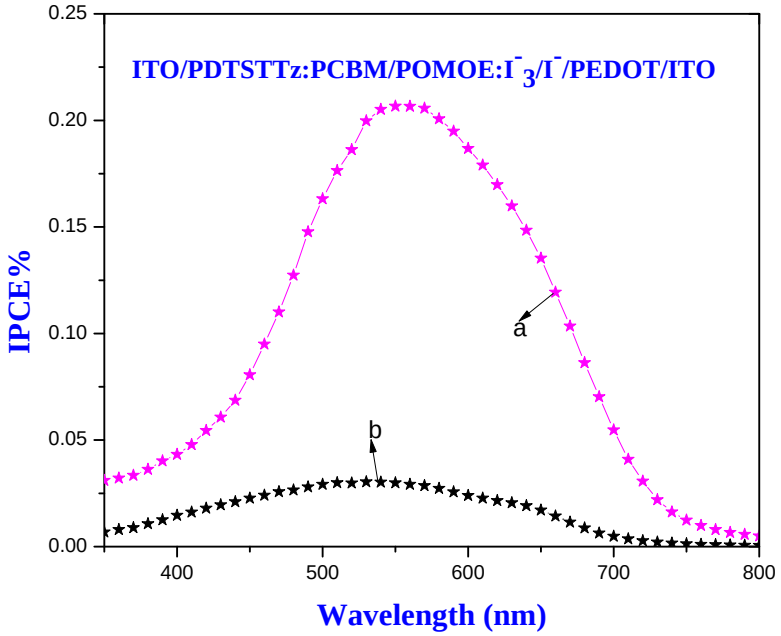
ITO/PDTSTTz:PCBM/POMOE:I-3/I-/PEDOT/ITO
IPCE%
Wavelength (nm)
a
b
0.25
0.20
0.15
0.10
0.05
0.00
400
500
600
700
800

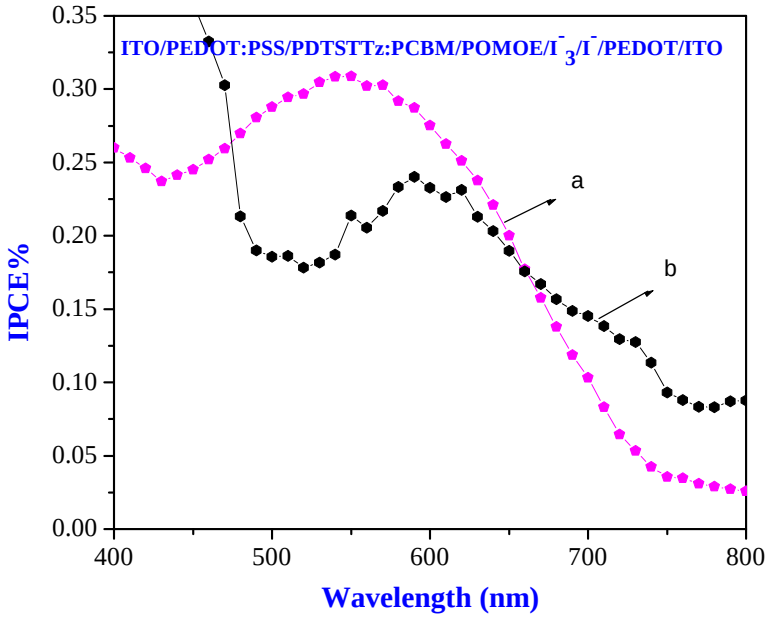
ITO/PEDOT:PSS/PDTSTTz:PCBM/POMOE/I-3/I-/PEDOT/ITO
IPCE%
Wavelength (nm)
a
b
0.35
0.30
0.25
0.20
0.15
0.10
0.05
0.00
400
500
600
700
800

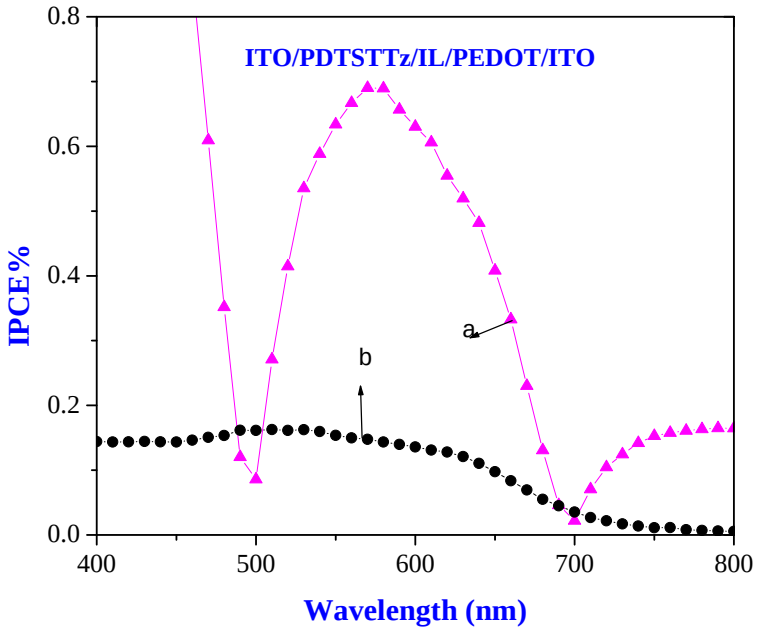

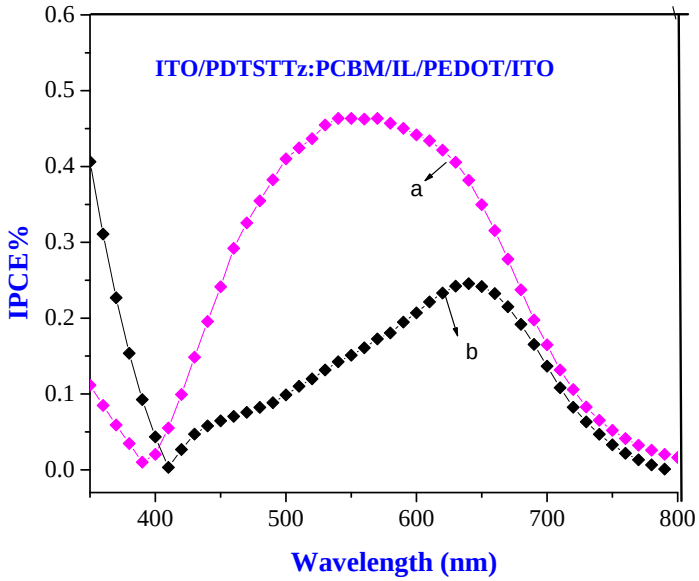

Figure 27: Photocurrent action spectra for different cells of PEC illuminated through (a) front side and (b) backside .

The figure showed that front side illumination resulted in higher conversion efficiency than backside illumination at the maximum absorbance. The reason behind this difference lies on the optical filtering effect of the polymer film. When light is illuminated from the backside, only a small fraction of the excitons produced by light absorption reach the interface to dissociate into carriers. Moreover, the presence of a high density of traps in the film reduces the number of carriers for the photocurrent generation. The greater the distance from the surface, the smaller is the probability for an excitons to reach the interface and dissociate into carriers [63].

The IPCE as a function of wavelength indicate that the conducting polymer gives rise to a photoresponse which is not limited in the region of its maximum absorption, the light harvesting effect can be observed in all the visible range.

Comparison of front side and backside photoresponses of different PECs are given in Table 3.

Table 3: Comparison of IPCE% of the different photoactive electrode on the front and back side illumination.

Photoactive electrode	**J_{sc} ($\mu A/cm^2$)**	**IPCE%**	**IPCE%**
		Front side	**Back side**
PDTSTTZ/ POMOE:I^-_3/I^-	1.4	1.9×10^{-2}	2×10^{-3}
PDTSTTz:PCBM/ POMOE:I^-_3/I^-	12.5	0.20	0.03
PEDOT:PSS/PDTSTTz:PCBM /POMOE:I^-_3/I^-	45.4	0.34	0.24
PDTSTTz/IL	78.5	0.69	0.16
PDTSTTz:PCBM/IL	95.6	0.46	0.24

When the J_{sc} of J - V and IPCE% are compared, they have a linear relation except the last two data, the reason behind this is in the case of a device PDTSTTz:PCBM as a photoactive electrode, the IPCE response is broad and the total current is a collective sum of each wavelength.

The conducting polymer exhibits photocurrent in practically all the visible range with a quantum yield less than 1%. In fact, recombination phenomena have great effect in organic materials due to their higher structural disorder.

Comparison of the optical absorption spectrum and spectral photo-response can be used to identify the active junction responsible for the photoelectrochemical phenomena. If illumination through the front side of the PEC produces a spectral response that corresponds to the absorption spectrum of the polymer film, then the polymer/electrolyte junction is responsible for the photoelectrochemical phenomena. Figure 28 shows the uv-vis absorption spectrum of the polymer film.

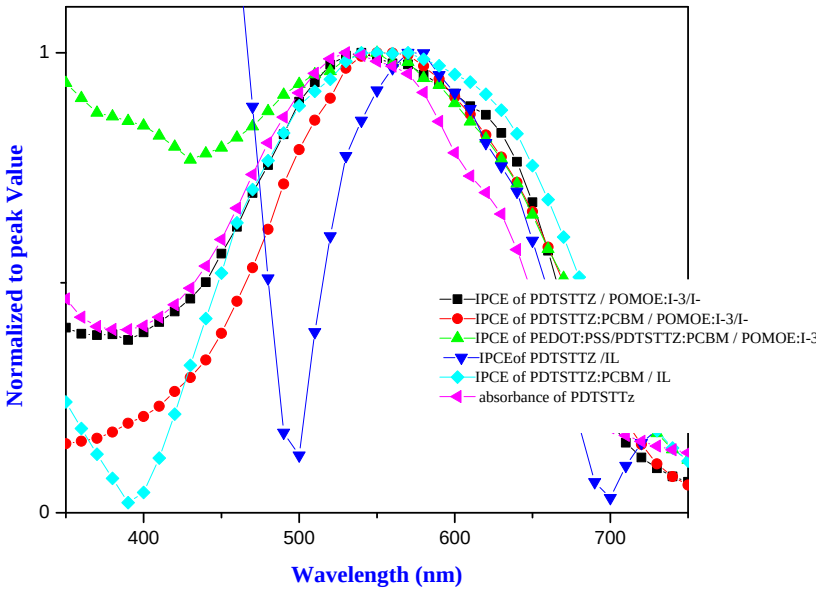

Figure 28: Normalized optical absorption spectrum of the film deposited on ITO and normalized action spectrum of different PECs for illumination through front side.

The normalized absorption spectrum of the polymer film as compared to normalized photocurrent action spectra of different cells of PECs for front side illumination are shown in Figure 28. The wavelength dependence of the IPCE% obtained from front side illumination closely resembles the absorption spectrum polymer film, which indicating that the photoactive junction is the polymer/electrolyte interface.

5.3 Transient Studies

Transient measurements of J_{sc} and V_{oc}, established during irradiation, are used confirm the generation of photocurrent of the PECs towards illumination through the front side with a light intensity of 100 $mWcm^{-2}$.

They were studied for all types of cells from the front side illumination. The short-circuit current density induced by the periodical blocking of the light path to the samples from the front side are shown in Figure 29.

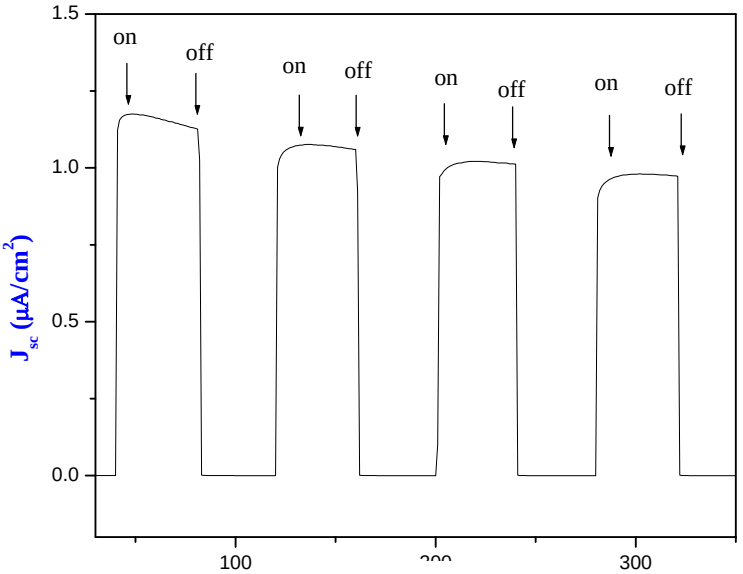

(a)

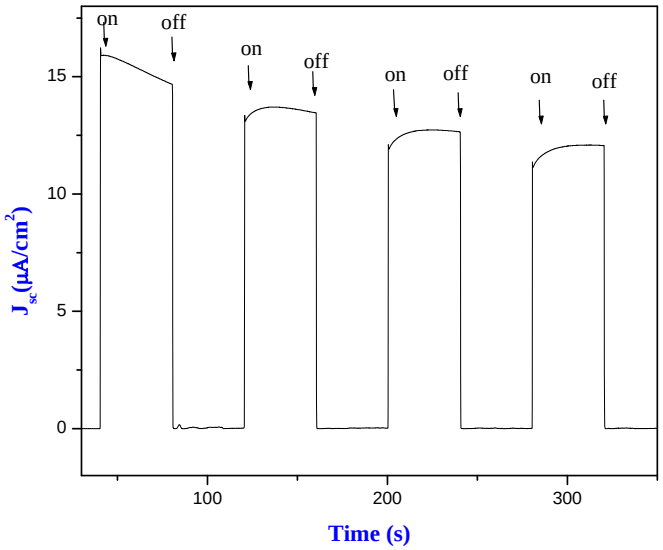
on
off
on
off
on
off
on
off
15
10
5
0
100
200
300
J sc (µA/cm2)
Time (s)

(b)

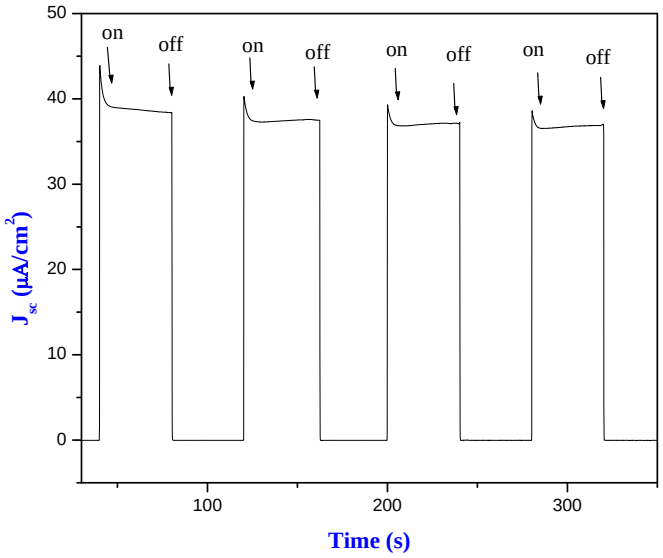
on
off
on
off
on
off
on
off
50
40
30
20
10
0
100
200
300
J sc (µA/cm2)
Time (s)

(c)

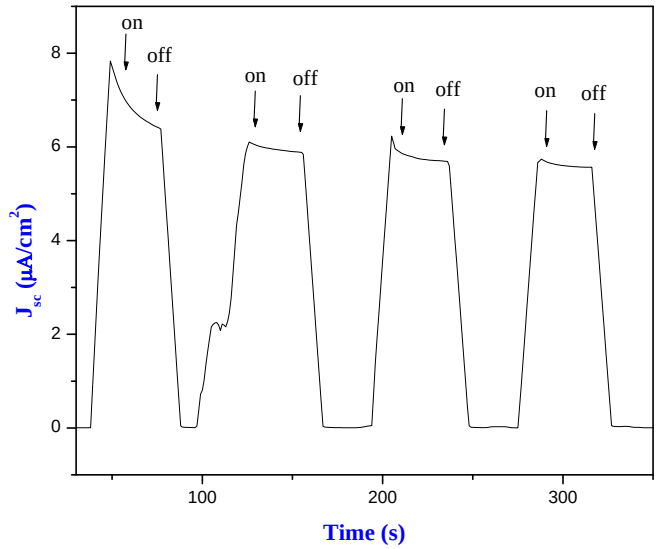

(d)

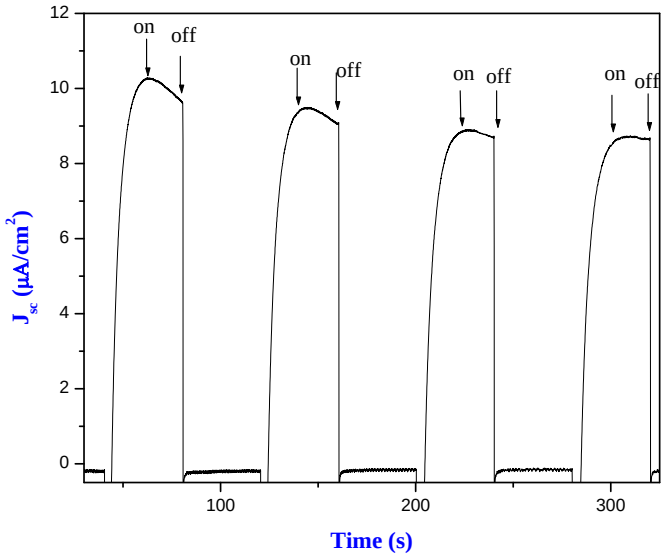

(e)

Figure 29: Short circuit current density response to switching illumination on and off from the front side of PEC cells with a light intensity of 100 mWcm^{-2} for a) ITO/PDTSTTZ/ POMOE:I^-_3/I^-/PEDOT/ITO, b) ITO/PDTSTTz:PCBM/ POMOE:I^-_3/I^- /PEDOT/ITO, c) ITO/PEDOT:PSS/PDTSTTz:PCBM/ POMOE:I^-_3/I^-/PEDOT/ITO d) ITO/PDTSTTZ/ IL/PEDOT/ITO and e) ITO/PDTSTTz:PCBM/ IL/PEDOT/ITO

All PECs shows a cathodic peak of photocurrent immediately after irradiation, with an exponential decay and stabilizing after a few second and reproducible when it induces repeatedly under several on and off cycles. This indicate that the devices generate photocurrent through illumination of light and there is no appreciable change in photocurrent with time of illumination. The decay indicates that recombination processes are occurring in the film, probably due to the presence of traps in the polymer bulk (mainly due to structural disorder).

The open circuit voltage induced by the periodical blocking of the light path to the samples from the front side are shown in Figure 30.

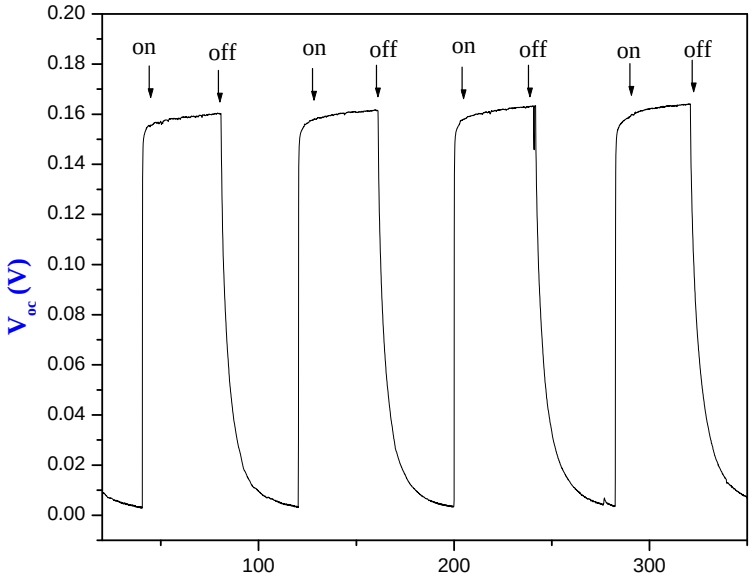

(a)

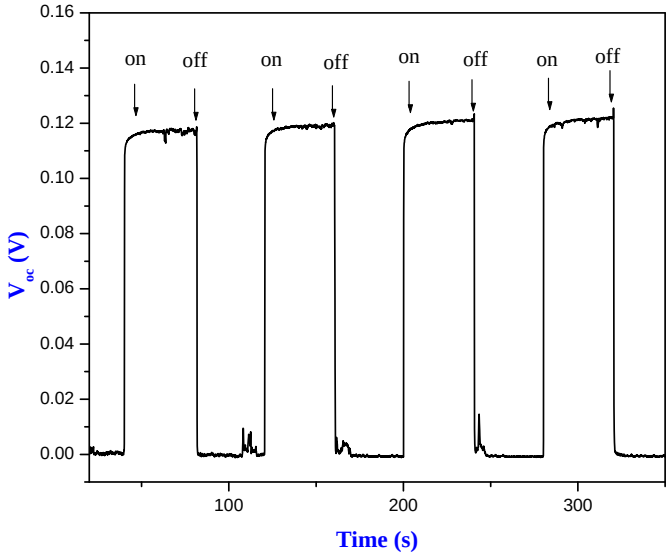
on
off
on
off
on
off
on
off
0.16
0.14
0.12
0.10
0.08
0.06
0.04
0.02
0.00
V oc (V)
100
200
300
Time (s)

(b)

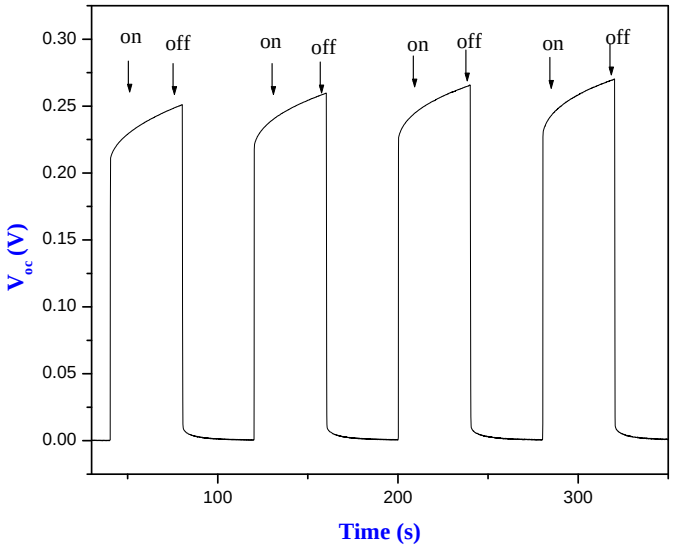
on
off
on
off
on
off
on
off
0.30
0.25
0.20
0.15
0.10
0.05
0.00
V oc (V)
100
200
300
Time (s)

(c)

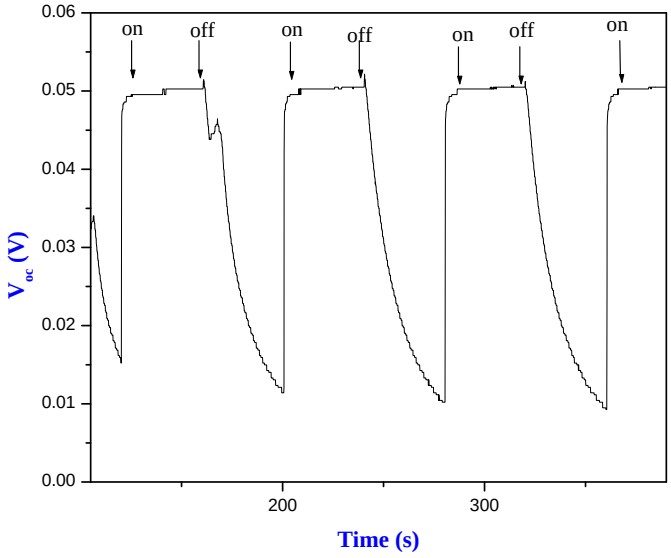

(d)

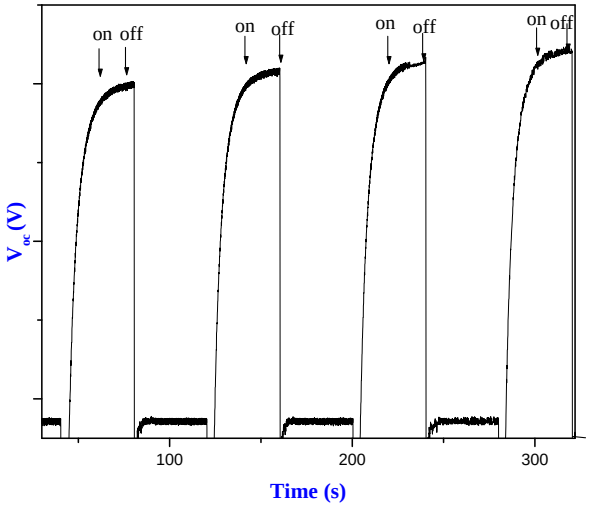

(e)

Figure 30: Open circuit voltage response to switching illumination on and off from the front side of PEC cells with a light intensity of 100 mWcm^{-2} a) ITO/PDTSTTZ/ POMOE:I_3^-/I^-/PEDOT/ITO, b) ITO/PDTSTTz:PCBM/ POMOE:I_3^-/I^-/PEDOT/ITO, c) ITO/PEDOT:PSS/PDTSTTz:PCBM/ POMOE:I_3^-/I^-/PEDOT/ITO d) ITO/PDTSTTZ/ IL/PEDOT/ITO and e) ITO/PDTSTTz:PCBM/ IL/PEDOT/ITO

The generation of open circuit voltage were characterized by a rise to a steady state value when the light is switched on and decay at approximately the same rate when the light is switched off. But for those device, which do not have an accepter , there is an exponential decay when the light is switched off which may be resulted in high recombination factor.

The short-circuit current density and open-circuit voltage obtained from the transient measurements were given in Table 4.

Table 4: J_{sc} and V_{oc} values obtained using transient studies.

Photoactive electrode	Transient study	
	J_{sc} ($\mu A/cm^2$)	V_{oc} (mV)
PDTSTTZ/POMOE: I^-_3/I^-	1.1	153
PDTSTTz:PCBM/POMOE: I^-_3/I^-	15.9	113
PEDOT:PSS/PDTSTTz:PCBM/POMOE: I^-_3/I^-	40.9	250
PDTSTTz/IL: I^-_3/I^-	8.4	48
PDTSTTz:PCBM/IL: I^-_3/I^-	10.2	22

6. Conclusions

In this study solid-state and quasi-solid state PECs were fabricated based on, PDTSTTz and a blend of PDTSTTz with PCBM photoactive electrode with a redox couple I^-_3/I^- and the I-V characteristics were studied. It has been shown that the device has converted optical energy into electrical.

In the case of all-solid state PEC, the J-V curve indicates that in addition to the accepter, adding a hole transporter, PEDOT:PSS layer, has lead to the increment of J_{sc}, V_{oc} and FF. The V_{oc}, the I_{sc} and the FF obtained for the solid-state PEC based on PEDOT:PSS/PDTSTTz:PCBM photoactive electrode were 311 mV and 45.4 μA/cm^2 and 0.34, respectively under illumination of white light with intensity of 100 mW/cm^2. Compared with all-solid state, a maximum photocurrent was harvested with scarification of open circuit voltage in quasi-solid state PECs. From the J-V curve it was confirmed that PDTSTTz behaves as p-type semiconductor.

The monochromatic photon to current conversion efficiency under illumination through front side for different cells at their maxima ranges from 0.0019% to 0.69%. The photocurrent action spectra study showed that the active junction for the photocurrent generation was that between the photoactive polymer and the redox couple.

From transient studies of J_{sc} and V_{oc}, the result show that the devices have a photo-response and they change solar energy in to electrical energy.

References

1. Sossina Haile, Susan M. Kauzlarich, Peter Battle, John Greedan, *Chem. Mater,* 22 **(2010)** 585.
2. D. Abbott, *Proceedings of the IEEE,* 98 **(2010)** 42**.**
3. T. M. W.J. Bandara, T. Svensson, M. A. K. L. Dissanayake, M. Furlani, W. J. M. J. S.R. Jayasundara, P. S. L. Fernando, I. Albinsson, B. E. Mellander, *J. Natn. Sci. Foundation SriLanka,* 41 **(2013)** 175**.**
4. Jun Chen, David L. Officer, Jennifer M. Pringle, Douglas R. MacFarlane, Chee O. Too, Gordon G. Wallace, *Electrochem. and Solid-State Lett.,* 8 **(2005)** A528.
5. M. Grätze, *Acc. Chem. Res.,* 42 **(2009)** 1788.
6. Tesfalidet Lemma, Teketel Yohannes, *J. Braz. Chem. Soc.,* 18 **(2007)** 818.
7. M. Grätzel, *Nature,* 414 **(2001)** 338.
8. Ana F. Nogueira, N. Alonso-Vante, Marco-A. De Paoli, *Synthetic Metals,* 105 **(1999)** 23.
9. Martin A. Green, Keith Emery, Yosihiro H., Wilhelm W., Ewan D. Dunlop, *Prog.in Photovoltics,* 22 **(2014)** 1.
10. S. A. Choulis, Y. Kim, J. Nelson, D. D. C. Bradley, *App. Phys. Lett.,* 58 **(2004)** 3890**.**
11. Gang Li, Rui Zhu, Yang Yang, *Nature photonics*, 6 **(2012)** 153 .
12. Maojie Zhang, Xia Guo, Yongfang Li, *Adv. Energy Mater,* 1 **(2011)** 557.
13. Marco-A. De Paoli, Wilson A. Gazotti, *J. Braz. Chem. Soc.,* 13 **(2002)** 410.
14. Jerry L. Reddinger, John R. Reynolds, *Adv. in polymer science,* 45 **(1999)** 58.
15. Hideki S., Edwin J. Louis, A. Macdiarmid, Chwank. C., A. Heeger *J. Chem. Soc. Chem. Comm*., **(1977)** 578.
16. V. Saxena, B. D. Malhotra ,*Current App. Phys.,* 3 **(2003)** 293.
17. W. R. Salaneck, R.H. Friend, J. L. Bredas, *Phys. Reports,* 319 **(1999**) 231.
18. S. A. Campbell, Y. Li, S. Breakspear, F. C. Walsh, J. R. Smith *Transactions of the Institute of Metal Finishing,* 85 **(2007)** 237.
19. Adam Pron, Patrice Rannou, *Prog. Polym. Sci*., 27 **(2002)** 135.
20. Herbert Naarmann. *Polym.,* **(2000).**
21. Hye-Ran Kang, Nam-Ju Jo, *High Performance Polym*., 18 **(2006)** 665.
22. Angew., *Chem. Int. Ed*., 40 **(2001)** 258.

23. A. Heeger, S. Kivelson, J. R. Schriefter, W. P. Su, *Rev. Modern Phys*., 60 **(1988)** 781.
24. Roberto M. Faria, O.N. Oliveira, *Braz. J. of Phys.*, 29 **(1999)** 360.
25. S. Srilalitha, K. N. Jayaveera , S. S. Madhvendhra, *Int. J. Innovative Res. in Sci., Eng. and Tech.*, 2 **(2013)** 2694.
26. Teketel Yohannes, Ph.D. dissertation, Department of chemistry, Addis Ababa University **1997**.
27. Kerileng M. Molapo, Peter M. Ndangili, Rachel F. Ajayi, Gcineka Mbambisa, Stephen M. Mailu, Njagi Njomo, Milua Masikini, Priscilla Baker, Emmanuel I. Iwuoha, *Int. J. Electrochem. Sci*. 7 **(2012)** 11859.
28. W. R. Salaneck, R. H. Friend, J.L. Bredas, *Phys. Reports*, 319 **(1999)** 231.
29. J.L.Breadas, G. B. Street, *Acc.Chem.Res.*, 18 **(1985)** 309.
30. P. W. M. Blom, M. C. J. M. Vissenberg , *Mat. Sci. Eng.*, 27 **(2000)** 53.
31. S. Kivelson, *Phys.Rev.*, B25 **(1982)** 3798.
32. B.E. Fenton , P.V. Wright, *Polym.*, 14 **(1973)** 589.
33. P. G. Bruce, C. A. Vincen, *J. Chem. Soc. Faraday Trans*., 89 **(1993)** 3187.
34. Pramod K. Singh, R. K. Nagarale, S. P. Pandey, H. W. Rhee, B. Bhattacharya, *Adv. Nat. Sci.: Nanosci. Nanotechnol*., 2 **(2011)** 13**.**
35. Jaipal Reddy. M ,CH. Ramesh , Siva Kumar. J, Subba Rao.U.V., *In. J. App. Eng. Res.*, 2 **(2011)** 147.
36. K. Ragavendran, P. Kalyani, A. Veluchamy, S. Banumathi, R. Thirunakaran, T. J. Benedict, *Portugaliae Electrochimica Acta*, 22 **(2004)** 149
37. Sisay Tadesse, Ph.D thesis dissertation, Department of chemistry, Addis Ababa University, 2012.
38. A.S. Ayesh, *Polym. Journal*, 41 **(2009)** 616.
39. Shao-Min Mai, Robert A. Colley, Jane H. Thatcher, Frank Heatley, Peter M. Budd, Colin Booth, *J. Mater. Chem.*, 6 **(1996)** 1099.
40. Walden P. *Bull. Acad. Imp. Sci. Saint. Petersburg*, 1800 **(1914)** 405.
41. Joon-Ho Shin, Wesley A. Henderson, Stefano Passerini, *J. Electrochem. Soc.*,152 **(2005)** A978.
42. Ling-Yu Chang, Chuan-Pei Lee, R. Vittal, Jiang-Jen Lin, Kuo-Chuan Ho, *J. Mater. Chem. A*1 **(2013)** 3055.

43. R. Kawano, M. Watanabe**,** *Chem. Comm*., 330 **(2003).**

44. Nageshewar D. Khupse, Anil kumar, *Indian J. Chem.*, 49 A **(2010)** 635.

45. Di Wei, Gehan Amaratunga, *Int. J. Electrochem. Sci*., 2 **(2007)** 897**.**

46. Arthur J. Nozik, *Ann. Rev. Phys. Chem.*, 29 **(1978)** 189.

47. Di Wei, *Int. J. Mol. Sci*., 11 **(2010)** 1103.

48. Teketel Yohannes, O. Inganäs, *J. Electrochem. Soc.*, 143 **(1996)** 87.

49. Teketel Yohannes, Theodros Solomon, O. Inganäs, *Synthetic Metals*, 82 **(1996)** 215.

50. Teketel Yohannes, J. C. Carlberg, O. Inganäs, Theodros Solomon, *Synthetic Metals,* 88 **(1997).**

51. Teketel Yohannes, O. Inganäs, *Synthetic Metals* 107 **(1999)** 97.

52. S. M. Sze , Kwok K. JOHN WILEY & SONS, INC., PUBLICATION, Third Edition , 2007.

53. A. Basu, Mohasin M. naqvi, T. K. Chakraborty, *Indian J. pure and App. Phys.*, 48 **(2010)** 899.

54. Francesco Greco, Alessandra Zucca, Silvia Taccola, Arianna Menciassi, Toshinori Fujie, Hiroki Haniuda, Shinji Takeoka, Paolo Dario, Virgilio Mattoli, *Electro. Sup. Information,* **(2011)** S1

55. Teketel Yohannes, O. Inganäs, *Sol. Energy Mater. Sol. Cells*, 51 (**1998**) 193.

56. L. Fan, S. Kang, J. Wu, S. Hao, Z. Lan, J. Lin ,*Energy Sources*, 32 **(2010)** 1559

57. P. Würfel, Physics of Solar Cells, Wiley-WCH, Weinheim, **2005**.

58. G. D. S. Saricifici, *Proceedings of the IEEE*, 93 **(2005**).

59. J. Roncali, *Acc.Chem. Res.*, 42 **(2009)** 1719.

60. Shawn Sapp, Silvia Luebben, *Appl. Phys. Lett*., 88 **(2006)** 152107**.**

61. Yijie Xia, Jianyong Ouyang, *J. Mater. Chem*,. 21 (**2011)** 4927

62. Yu-Kai Han, Mei-Ying Chang, Wen-Yao Huang, Hsin-Yu Pan, Ko-Shan Ho, Tar-Hwa Hsieh, Sin-Yu Pan, *J. Electrochem. Soc*., 158 **(2011)** 88.

63. A. K. Ghosh, T. Feng, *J. Appl. Phys*., 49 **(1978)** 5